Optimization of Ship Hull Based on Wave Making Resistance

by

©Md Shahriar Nizam

A Thesis submitted to the School of Graduate Studies in partial fulfillment of the requirements for the degree of

Master of Engineering

Faculty of Engineering and Applied Science

Memorial University of Newfoundland

October 2016

St. John's Newfoundland

Abstract

A numerical program is developed to optimize the ship hull based on wave making resistance. Ship hull geometries are modified to optimize the hulls within a limit to maintain the design criteria. In this work, a non-uniform rational b-spline (NURBS) based hull surface is taken as the input for optimization. MAPS resistance is a potential theory based program that uses a modified Dawson method to calculate wave making resistance. An automatic hull discretization system is developed for calculating wave making resistance by MAPS resistance. Two different algorithms, Path of steepest descent (PSD) and Broyden–Fletcher–Goldfarb–Shanno (BFGS) are employed for optimization. At first the PSD is used for optimization. Later on a BFGS algorithm is applied with the help of a Kriging technique to reduce the computational time and expense. Three different kinds of hull modification methods are introduced to optimize the ship hull. Multiple ship hulls are used for validating the optimization technique. All the ship hulls produced satisfactory results by decreasing the wave making resistance. The optimal hulls are further investigated for a series of Froude numbers to compare their wave making resistance with published experimental data.

Acknowledgements

Foremost, I would like to give my highest esteem and thanks to my supervisor, Prof. Heather Peng for her invaluable academic guidance with patience and kindness throughout my studies. Her guidance helped me in all the time of research. I would like to thank her for giving me an opportunity to work under her supervision. I also like to thank Dr. Wei Qiu for teaching me marine hydrodynamics and giving me an opportunity to work on diverse exciting projects within the Advanced Marine Hydrodynamic Lab (AMHL).

I would like to thank Dr. Shaoyu Ni for his continuous support on my work. I am also grateful to Dr. G. C. Bohling of Kansas Geological Survey for his valuable suggestions on my work. I am indebted to Dr. Michael Hinchey for his continuous support in my graduate life. My appreciation is extended to NSERC CREATE Training Program and School of Graduate Studies for financial support during my studies.

I would also like to acknowledge Dr. Bruce Colbourne and Dr. David Molyneux at Memorial University as reviewers of this thesis, and I am indebted to them for their valuable comments on this thesis.

I owe deepest gratitude to my friend Hossameldeen Bakr for his continuous support and unconditional friendship in my graduate life. I would like to thank my fellow lab mate Junshi Wang in AMHL Group for helping me in writing this thesis. I am indebted to many of my colleagues to support me. Among them I would like to

mention the names of Boyang Zhang, Mihajlo Ćurčić, Mohamed Karam, Mahmoud Essam and Md Ashim Ali. I would like to thank Moya Crocker, Colleen Mahoney, and Nicole Parisi in the graduate studies office who have greatly assisted and guided my graduate life in Memorial University. I am grateful to everyone who has contributed to this work and helped me during my studies.

Last but not the least, I would like to thank my parents for their unconditional love, understanding, and support throughout my studies and my life as well.

Table of Contents

List of Tables

List of Figures

Nomenclature

$[B]$	Hessian Matrix
b_i	Coefficient of regression
BBD	Box-Behnken design
BFGS	Broyden Fletcher Goldfarb Shanno
C(t)	Curve created by NURBS
c_0, c_1, c_2	coefficients of semivariogram
CCD	Central composite design
C_w	Wave making resistance coefficient
g	Gravitational acceleration
k, l	Number of parameters along U and V direction
m, n	Total number of control points along U and V direction
$N_{j,p}$	B-spline basis function
NURBS	Non-uniform rational basis spline
PSD	Path of steepest descent
p, q	Degree of curves
P_j	Coordinate of control points on curve
P_k	Directional Matrix in BFGS algorithm
$P_{i,j}$	Coordinate of control points on surface
R_w	Wave making resistance of ship

RSM	Response Surface Method
t, r	Parameters of surface along U and V direction
s	Location of a field point for kriging
S	Wetted surface area
U_0	Forward speed of ship
U, V	Two dimensional parametric coordinate system
$\mathbf{U}, \mathbf{V}$	Knot vector along U,V direction
w_j	Weight of control points
x, y, z	Coordinate of point along X, Y and Z direction
X, Y, Z	Three dimensional Cartesian coordinate system
$Y(s)$	Predicted response of a field point 's' due to kriging
$\in$	Random experimental error
$\in_{ki}$	Difference between predicted and actual value at any field point
σ^2	Variance of error
γ	Semivariogram
Γ	Corelational function
ϕ_L	Lagrangian function
$\bigtriangledown f(x)$	Derivatives of function f(x)
α	Step length in line search method
ϕ	Total velocity potential
Φ	Velocity potential
φ	Distributed velocity potential
$\overrightarrow{n}$	Outward normal vector from the ship hull
η	Free surface elevation
ρ	Water density

Chapter 1

Introduction

1.1 Background

Ship design is one of the most important stages of ship construction. Although this is done in a very preliminary stage, it has a significant effect on the ship's entire life. Not only that, seakeeping performance is also determined by the ship hull design. Ships consume large amounts of fuel in their operation. As a result, ships emit unfavorable gases like CO_2, $H_2O(aq)$, NO_2, NO_3, SO_3 etc in the environment. In 2011, the International Maritime Organization (IMO) introduced a new rule to reduce greenhouse gases emission for ships (MARPOL Annex VI, Chapter 4). This regulation has been effective since January 2013. As a result, it has become mandatory to limit the emission of toxic gases from ships. The total resistance of a ship mainly consists of viscous resistance and wave making resistance. For low speed the viscous resistance dominates but with the increase of ship speed the wave making resistance becomes dominating. So for ships with higher speeds, it is essential to reduce the wave making resistance in order to reduce the total resulting resistance. For these reasons, it is crucial for a ship hull design to be optimized. In this thesis, the main target is to

reduce the wave making resistance by optimizing ship hull geometry.

1.2 Literature Review

The geometry of ship hull is complex. To optimize a ship, it is required to represent the hull mathematically. Besides this, selecting the region of optimization and selecting the types of optimization make the whole optimization procedure difficult. The total optimization procedure for a ship can be divided into hull representation, hull deformation, and optimization procedure.

1.2.1 Hull Representation

Ship hull shapes are difficult to represent by mathematical equations. Due to the complexity of ship hull, no mathematical formula has been established to represent commercial ship hull perfectly. For this reason it is challenging to modify an established hull shape as per requirement. In early days, ship design researchers used the offset table of the ship to represent the hull form. The benefit of using the offset table is that it is relatively easy to use and understand. To solve these problems, researchers started to use Bezier curve to represent the hull. Bezier curve is very simple to use and provides good representation of the geometry. But this curve has some major drawbacks. Increasing degree of a Bezier curve adds flexibility to the curve but at the same time it also increase the processing effort and probability of causing numerical noise in calculation. Beside these the Bezier curve requires more control vertices to define the curve properly and joining two Bezier curves is relatively complex. To overcome these problems, spline curve was introduced. There is a wide range of splines. The most popular one is the cubic spline. Spline is a numerical function that is piecewise continuous and its shape is defined by a polynomial function. Recently the B-spline

has become very popular for surface representation. It can give a clear mathematical expression of ship hull. In this method the points on the B-spline surface are very close to the original control points. As a result it gives very accurate information about the ship hull. Rogers (1980) gave a detail discussion about the procedure of generating a hull using B-spline surface. Park and Choi (2013) used B-spline based surface modeling technique during the optimization procedure. Although the B-spline gives very good representation of geometry, it has some drawbacks. B-spline curves are variant under transformation. Beside this this curves are unable to define conic sections. To fix these problems a modified version of B-spline is introduced, known as Non-Uniform Rational B-spline(NURBS). In NURBS the user has better authority over the control points as they are governed by weights.

Researchers frequently uses the NURBS based hull representation. Kim et al. (2008) described a CFD based optimization procedure where the input of the geometry is NURBS surface. Ping et al. (2008) used a new way of hull generation based on NURBS surface.

With the help of B-spline and NURBS, parametric modeling is introduced. This design-oriented parametric definition language is introduced to vary ship hulls quickly and smoothly. By using the parametric modeling Harries (1998) developed a method based on global and regional form parameters such as principal dimensions, different coeffcients etc. In the surface generation part he used a set of B-spline curves to represent the sectional curves of the ship hull. Later on this method is modified by Abt et al. (2001). They presented a parametric modeling approach that is fast and efficient to produce multiple hull at the time of hull variation. Ping et al. (2008) introduced another quick approach to generate and variate hull based on parametric hull generation. Han et al. (2012) described a fairness optimized B-spline form parameter curve based hull variation procedure by applying parametric hull design.

The benefit of using this technique is that based on the selected parameters, the hull form modification can be done very easily and results in smooth surfaces. The main problem with this procedure is that making a parametric model for complex geometry is not easy. It requires higher skill and adequate time to generate a accurate model. To avoid this problem, the NURBS based ship model is used in this work as an input hull geometry, which is relatively easy to generate and more available.

1.2.2 Hull Modification

The types of hull modification procedures for ships can be divided into three parts: global, regional, and local (Nowacki et al. (1995). There are numerous methods regarding global modification. Shifting the stations of the hull along longitudinal direction is one of the major and popular global modification procedures. Ground breaking work on modification of ship hull design by shifting the sections was carried on by Lackenby (Lackenby (1950)). In his work he modified the hull by modifying the position of the longitudinal center of buoyancy, by varying the fullness of the hull and by changing the length of the parallel middle body of the ship. Lackenby introduced shift functions to change the existing position of hull sections by keeping the fore and aft perpendiculars unchanged. Janson and Larsson also introduced another procedure of hull modification based on two different types of variable (Janson and Larsson (1997)). For the modification of the hull they used a program known as ALADDIN, which is capable of varying the hull geometry based on two parameters, master and slave. Slave is a function of master parameters. They optimized the hull globally based on the ship resistance. Markov and Suzuki modified the ship hull globally based on the shifting of mathematically generated surface sections and real ship sections (Markov and Suzuki (2001)). In their work they also introduced another procedure based on shifting and deforming of real ship sections. Grigoropoulos introduced a global hull

variation by changing the dimensions from a parent hull (Grigoropoulos (2004)). In their work the hull with best seakeeping behaviour is selected based on a weighted sum of the resonant values. Once the hull is selected it can be modified locally to improve the optimizing property. In this thesis a global modification is carried out based on a shifting method. This procedure is similar with Markov's shifting of mathematically generated surface sections, but with the exception that the amount of shift on forward and aft regions can be controlled by two parameters. This allows the ship shape to remain undistorted while the hull is undergoing variation.

In the regional modification procedure, a ship hull is deformed regionally instead of globally. A certain portion of the hull goes through the modification algorithm to produce a new hull surface. Regional surface modification can be done by using Markov's shifting procedure(Markov and Suzuki (2001)). But this shifting only works on a certain portion of ship hull. Park and Choi (2013) introduced a regional deformation by modifying the B-spline surface of a certain portion of ship. In the works of Kim et al., a new regional shifting method is frequently used. In their multiple papers they used a custom formulation to modify the sectional area distribution of a ship (Kim and Yang (2010b), Kim et al. (2010), Kim and Yang (2013), Kim and Yang (2011)). This method is also used in this thesis for surface modification.

Local hull modification indicates deforming certain points on a ship's hull. The hull deformation can be carried out locally by modifying the control points on the bow, stern, and combination of both (Kim et al. (2008), Kim and Yang (2010a), Kim and Yang (2013)). The other way of modifying the hull locally is moving some control points on the surface (Janson and Larsson (1997)). The advantage of local modification is that in this way modification can be done on any place of the ship but because of this kind of flexibility it also creates an unrealistic change in the shape of ship hull. As a result hull fairing is required to be done at the time of local optimization. In this

work, beside the global and regional deformation, another hull deformation is also carried out. It is actually a local deformation procedure, but as result of this kind of modification, a certain region is required to be modified. Beside these three modification procedure, another new approach is also used by researchers. It is parametric design based modification. Though the representation of hull by parametric design is complex, it has advantages for hull variation. Once a hull is defined by parametric design, it can easily be deformed with high precision.

Hollister used four methods for ship hull modification. These are the stretching method, balancing method, Lackenby method and CMVARY method (Hollister (1996)). In the stretching method, the ship hull is varied based on the principal dimensions. In balancing method, a couple of parameters are changed but the remaining parameters are modified as per the variables to reduce the effect of the variables. The Lackenby method shifting technique is implemented by varying the ship hulls and in the CMVARY method the midship of the ship is kept variable.

1.2.3 Optimization Methods

The choice optimization methods plays a pivotal role in ship hull optimization. Different optimization methods have different types of advantages and disadvantages. Generally the efficiency of an optimization procedure depends on the number of runs before getting the optimized value. Beside this, complexity and total time required for each run are also issues. A typical optimization problem can be stated as follows.

$$\text{Find variable } X = \begin{Bmatrix} x_1 \\ x_2 \\ \vdots \\ x_n \end{Bmatrix} \qquad \text{which minimize or maximize the function f(X)}$$

The objective function f(X) can be subjected to the equality and inequality constraints. Based on the type of objective functions, the equality and inequality constraints can be written as follows.

$$\text{Inequality constraint: } g_i(X) \leq 0; \qquad \text{i} = 1, 2, ..., \text{m}$$

$$\text{Equality constraint: } h_j(X) = 0; \qquad \text{j} = 1, 2, ..., \text{n}$$

where, m and n are two positive numbers those depend on the type and requirement of the problem.

The present study is focused on reducing wave making resistance of a hull form. If the wave making resistance coefficient at a particular speed of the initial hull and the hull obtained during the optimization process are respectively C_w^i and C_w^d, the objective function $f(x)$ can be defined as follows:

$$f(x) = \frac{C_w^i - C_w^d}{C_w^i}$$

The optimization procedure can be divided into deterministic methods and heuristic methods based on techniques applied for optimization. The classical methods for solving optimization problems are deterministic methods. In these methods normally hessian or gradient calculation is required, resulting in increasing the complexity of the procedure. The procedures are relatively complex to calculate but they also provides a very detailed information about each step of the optimization. Deterministic based optimization like Sequential Quadratic Programming and Quasi-Newton methods can handle large-dimensional problems. The conjugate gradient method uses gradient to find the optimal result. For constrained optimization, interior point method give fairly acceptable results although it can not reach the optimum point of problem. Gradient

descent method uses the gradient to find the steepest path to reach the maxima/minima. Beside these methods there are some other popular deterministic methods such as sub gradient method, bundle method of decent, ellipsoid method and reduced gradient method and many more.

Heuristic methods are a technique designed for reducing searching problem-solving activities and are a means to obtain acceptable solutions within a limited computing time (Zanakis, 1981). The solution from these methods may not be the best solutions but they are among the reasonable solutions. The main advantage of these methods are that like deterministic methods it does not need longer time to achieve the optimized results and generally it takes less run than the deterministic methods. Besides this advantage, heuristic methods normally do not contain any derivatives for calculation resulting a simple procedure for optimization. At the time of using heuristic optimization methods some properties require to be traded off. In some problems, there is more than one solution. Heuristic methods do not provide guarantee for giving the best solution among these solutions. Again sometimes there are more than one solutions in a problem. These methods are not able to find all the solutions. Accuracy is another major trade off for heuristic algorithms. As these techniques cannot find all the solutions, so it is quite uncertain to predict the accuracy of an optimized solution obtained by heuristic methods. There are some popular heuristic methods that can provide approximate solutions to optimization problems. Mimetic algorithm, Evolutionary algorithms, Genetic algorithms, Hill climbing with random restart, Particle swarm optimization, Artificial bee colony optimization, Simulated annealing, Tabu search etc. are among them.

Based on the types of problems and hull variation, researchers use different optimization methods. Markov and Suzuki (2001) introduced hull modification technique by shifting the hull section and deforming the ship geometry. They preferred a deter-

ministic method known as Davidson-Fletcher-Powell (DFP) for optimization. Chun (2010) used gradient-based sequential quadratic programming (SQP) for reducing wave making resistance that provide acceptable results for local optimization. In his work, a parametric design based hull was introduced to vary the hull geometry. Saha et al. (2004) optimized the resistance of a ship hull by multiplying the breadth of the ship hull with a coefficient by using SQP. Park and Choi (2013) also adopted this optimization method to reduce the resistance of a ship by using a CFD technique. In their works, they used multiple variables to variate the ship hull. The benefit of SQP is that it can handle any degree of non-linearity including non-linearity in constraints. The main disadvantage of this method is that it contains multiple derivatives which need more time and work as well. Partial swamp optimization (PSO) is metaheuristic procedure. This method does not need any derivative to optimize a problem, as a result it is a less complex method than most of the other methods. The benefit of this method is that it can search very large spaces of variable solutions but at the same time it does not ensure that optimal solution is found. Although having this drawback, researchers uses this method because of the simplicity of this method. Chun (2010) also used PSO method to optimize the ship hull along with SQP.

More recently, there is another popular optimization method known as genetic algorithm (GA). This method is a heuristic method based on the idea of Darwin's natural selection theory. Like natural selection theory, this method also contains inheritance, mutation, selection, and crossover to obtain the optimal value. Mahmood and Huang (2012) optimized the bulbous bow of the ship to reduce the total resistance of ship by using a genetic algorithm. In that work they varied the shape of bulbous bow by changing the bulb parameters based on genetic algorithm. Kim et al. (2008) and Kim and Yang (2010b) have carried out CFD based optimization where the applied method was a genetic algorithm. More works on ship hull optimization are done by

Kim et al. (2010), Matulja and Dejhalla (2013) and Bagheri et al. (2014). Although as a heuristic method GA has capability of versatile applicability, it has also some demerits. Genetic algorithm usually takes longer time than other optimization methods. But researchers are using it widely because of its capability of versatile applicability. In the present work at first a deterministic optimization algorithm known as path of steepest descent is introduced. The target of this algorithm is move along the region in which the process generates improved result. This is a straight forward and easy to implement method. With the increment of variables this method takes huge computational time. To avoid this problem a gradient based optimization method known as BFGS (Broyden-Fletcher-Goldfarb-Shanno) has been adopted that is an advanced unconstrained optimization algorithm. This method can be considered as quasi-Newton, conjugate gradient and variable metric method.

1.3 Statement of the problem

The objective of this study is to develop a practical NURBS based calculation tool for the hydrodynamic optimization of ship hull forms for reducing wave making resistance at the early stage of design. To calculate the wave making resistance a panel based wave making resistance calculation tool known as MAPS-Resistance is used. The input for MAPS Resistance is ship hull surface panels. So a program is required that can generate ship hull geometry in terms of panels from NURBS. At the time of ship hull optimization, the hull geometry will go through a continuous modification based on the optimization code. So it is also required to make sure that after each modification the program will also generate suitable panels for calculating the wave making resistance. Based on the step length of the optimization, the program may need to calculate the wave making resistance more than a thousand times which is

cost ineffective and time inefficient. To avoid this problem, a surrogate based model is required for mimicking the whole scenario. After the surrogate model is constructed, an optimization solver is required to find the optimal ship hull. In the following section, the framework of the computational program will be discussed.

1.4 Thesis Content

In this thesis, chapter 1 provides literature review of the work and at the same time it also give a clear idea about the statement of the problem. In chapter 2, a theoretical description of NURBS, Kriging, optimization and wave making resistance are provided. In chapter 3, multiple methods for surface unification, grid generation and three different kinds of hull variation procedures are introduced. Chapter 4 shows the outcome of the optimization procedure for Wigley, Series 60 and KCS container hull. Finally chapter 5 gives conclusion and recommendation for future research.

The goal of this research is to develop a numerical tool to predict the optimized ship hull on the basis of wave making resistance. In this procedure the optimization starts with grid generating from an IGES file. Then path of steepest descent is used for optimization. To avoid huge time consumption, later on Kriging method is introduced to predict whole optimization scenario. Finally BFGS algorithm is used to find the optimized ship hull. The work procedure with PSD and BFGS can be illustrated by two separate flow chart as follows.

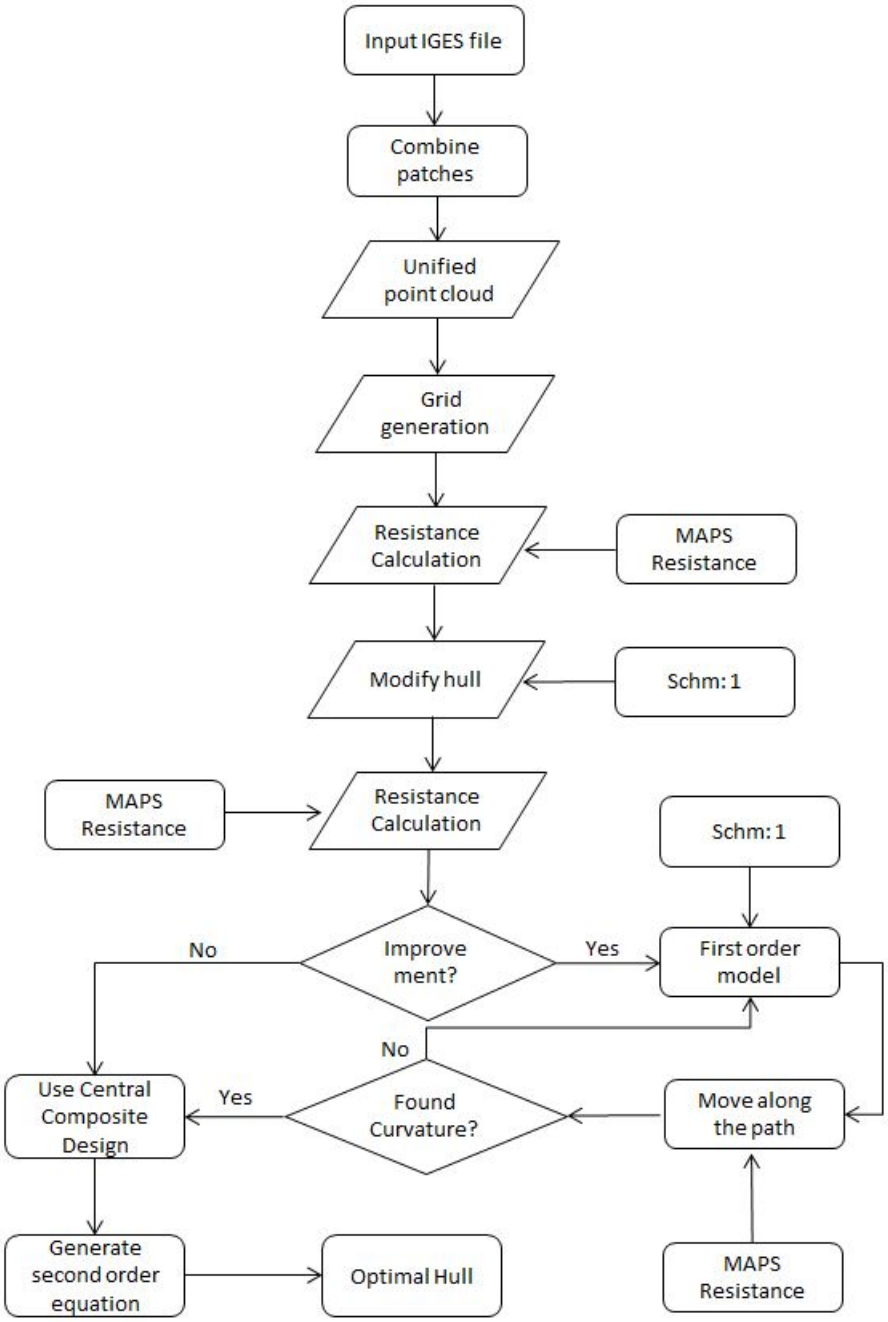

Figure 1.1: Flowchart of work procedure with path of stepeest descent

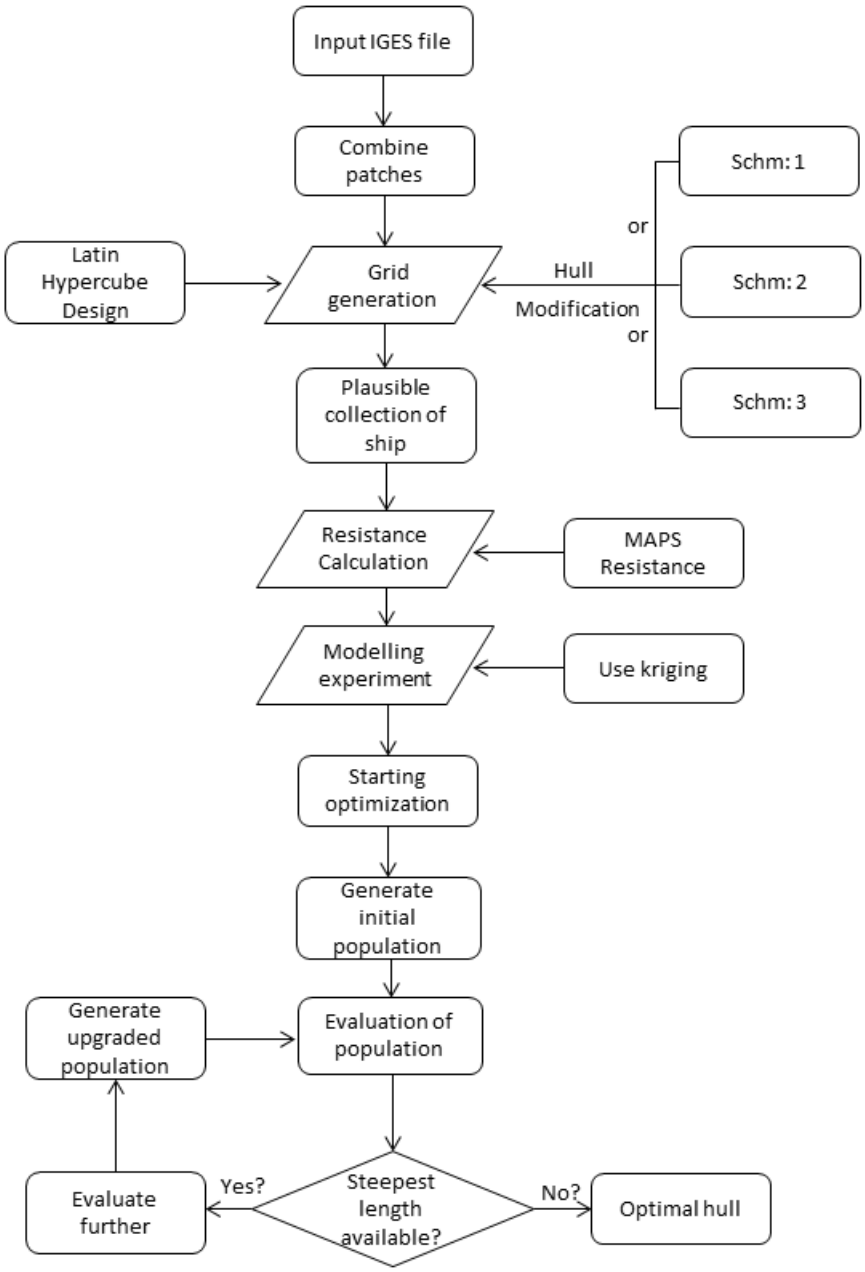

Figure 1.2: Flowchart work procedure with BFGS

Chapter 2

Mathematical Formulation

The hull of ship is a very complicated three dimensional shape. For the ease of calculating properties, it is very common to use mathematical equations to represent a geometry. As the shape of ship is complex, ship designers give high emphasis on the graphical description of hull forms. In the past, a ship's hull form is represented graphically by lines plan. The lines plan consists of projections of the intersection of the hull with XY,YZ and ZX directional plane. A typical linesplan with offset table is provided in figure 2.1, where body plan, half-breadth plan and sheer planes are indicating the stations, waterlines and buttock lines of ship. The geometry of the hull is represented by the table of offset. To represent ship hull different types of curves and surfaces like Hermit interpolation, Bezier curves, Spline, B-spline and recently non uniform rational basis spline(NURBS)are introduced. Among these methods, NURBS gains popularity and usability because of its flexibility and precision for handling. A typical graphical representation of surface by NURBS is depicted on figure 2.2. For transferring the information of surface electronically, different types of file format are used. Among all the formats, IGES file format is one of the very common digital file formats that allows exchange of information among computer-aided design (CAD)

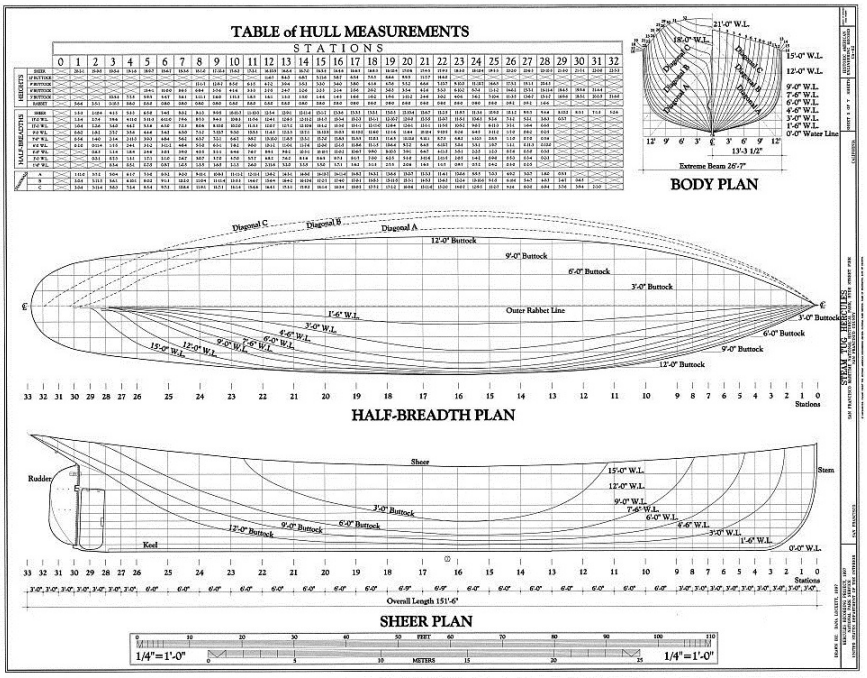

Figure 2.1: Typical lines plan of a utility ship(www.themodelshipwright.com)

systems.

In this thesis, the optimization of ship hull is carried out from an input ship geometry. To get precise information about the ship, IGES file format is used as an input. After getting the surface information, the appropriate panel distribution for calculating wave making resistance is created by a panel rearranging method. A convergence test is carried out to find suitable number of panels for the calculation of wave making resistance. Later on the method of steepest descent is introduced to get minimum resistance. This procedure works well but the main problem is that the required number of iterations can be more than couple of hundreds in this approach. Depending on the step size the number of run can be more than thousand times. It is a time consuming and cost ineffective process. To overcome this problem a process known as optimization based on Kriging method is introduced. The main benefit of the Kriging method is that once we have our database or field points, we can easily find the minimum point based on the optimization. After generating a model from Kriging a improved

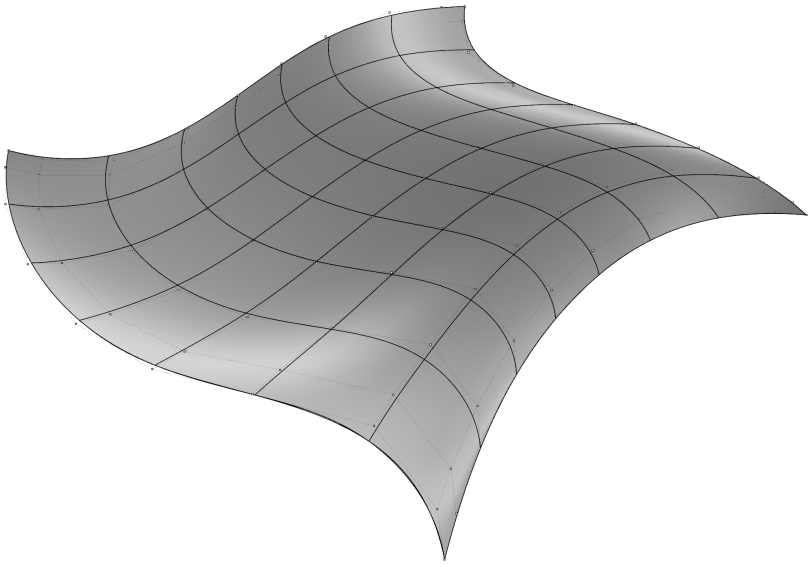

Figure 2.2: Graphical representation of NURBS surface

optimization procedure, Broyden Fletcher Goldfarb Shanno(BFGS) algorithm is used to find the optimal resistance. The detail mathematical formulations are provided is the following parts of this chapter. The whole procedure can be divided into four parts.

- Surface point generation
- Developing Kriging model
- Optimization
- Wave making resistance calculation

2.1 Surface Point Generation

2.1.1 Non Uniform Rational B-spline Surface

The structure of an IGES file is consists of five parts: Start, Global, Directory Entry, Parameter Data, and Terminate. Among these five parts the characteristics and geometric information for any geometry is provided on directory Entry and parameter data. A typical example of IGES file is provided on Appendix A.1. The parameter data section contains the information about the NURBS. A NURBS curve ($C(t)$) can be defined as (Piegl and Tiller (1997)):

$$C(t) = \frac{\sum_{j=0}^{m} N_{j,p}(t) w_j P_j}{\sum_{j=0}^{m} N_{j,p}(t) w_j} \tag{2.1}$$

where, $N_{j,p}(t)$ = p−th degree b-spline basis functions based on knot vectors, w_j= weights of the control points, t = parameters of the curve, P_j = coordinate of control points, p= degree of the spline and m = total number of control points on a curve.
In NURBS, a knot vector defines how the basis function will behave at different positions along a curve. It controls the continuity between the different arcs of the basis functions. It also determine where and how the control points will affect the curve. The number of knots are always equal to the number of control points plus curve degree plus one. Generally there are two types of knot vectors, clamped and unclamped. These two types can be subdivided into uniform and nonuniform knot vectors. For a second degree curve containing six control points if the knot vectors are defined by **U**, an example of different types of knot vectors can be provided on equation 2.2.

$$\mathbf{U} = \begin{cases} 0,0,0,1,2,3,4,4,4 & \text{:Clamped Uniform} \\ 0,0,0,2,5,6,7,7,7 & \text{:Clamped Nonuniform} \\ 0,1,2,3,4,5,6,7,8 & \text{:Unclamped Uniform} \\ 0,0,1,2,4,5,5.5,7,8 & \text{:Unlamped Nonuniform} \end{cases} \tag{2.2}$$

There are different methods for calculating parameters for NURBS. Among them three common methods are equally spaced parametrization, chord length parametrization and centripetal method parametrization. Each of these procedures has some benefits and some limitations. The main benefit of using equally spaced parametrization is that it is very simple and easy to use but it can produce erratic shapes if the control points are distributed in bumpy pattern. To avoid this problem chord length parametrization is introduced. For most of the cases this method is adequate but for further improvement centripetal method can be used (Piegl and Tiller (1997)).

In this work at first the equally spaced parameter is taken for generating the parameters. Later on equal chord parametrization is also used. But using the second method did not improve the surface representation as the points of input files are distributed in an organized way. The input data are taken from the IGES file where data are organized enough to give good results using the equally spaced method. The equally spaced parameter can be calculated by equation 2.3 (Piegl and Tiller (1997)).

$$t_1 = 0,\ \ t_n = 0\ \ and\ \ t_i = \frac{i}{n},\ i = 2,3,4,...,(n-1) \tag{2.3}$$

where, t= parameter, n= number of parameters. The chord length parametrization can be represented by equation 2.4 (Piegl and Tiller (1997)).

$$t_1 = 0,\ \ t_n = 0\ \ and\ \ t_i = t_{i-1} + \frac{\mid C_i - C_{i-1} \mid}{d},\ i = 2,3,4,...,(n-1) \tag{2.4}$$

where, $d = \mid C_i - C_{i-1} \mid$, t= parameter and n= number of parameters.

The weights (w) of the control points determine the effect of points on the curve. Generally the weights are positive numbers. For a curve if all the control points have the same weight, the curve is known as non-rational curve, otherwise the curve is called as rational curve.

Once the knots, weights and parameters are calculated, the basis function $N_{i,p}$ can be calculated based on a recurrence formula known as deBoor′s algorithm (Piegl and Tiller (1997)). For the $(l+1)$ number of knots, n number of points and p-th degree spline, the formula of B-spline basis function can be described by equation 2.5 and 2.6.

$$N_{j,0}(t_k) = \begin{cases} 1 & \text{if } u_j \leq t_k < u_{j+1} \\ 0 & \text{otherwise} \end{cases} \tag{2.5}$$

$$N_{j,p}(t_k) = \frac{t_k - u_j}{u_{j+p} - u_j} N_{i,p-1}(t_k) + \frac{u_{j+p+1} - t_k}{u_{j+p+1} - u_{j+1}} N_{j+1,p-1}(t_k) \tag{2.6}$$

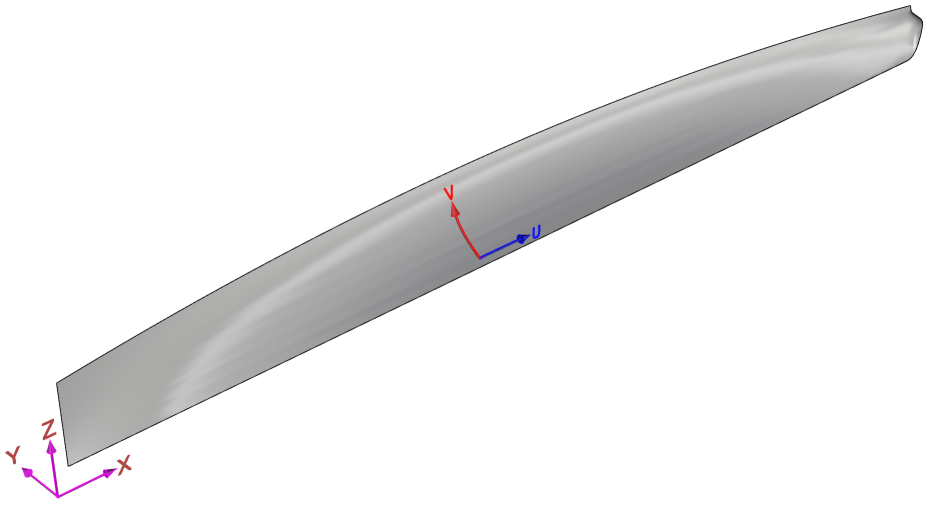

Figure 2.3: Dimensional and non dimensional coordinate system for ship

In figure 2.3, the coordinate system for ship is introduced where X,Y and Z indicating the direction of cartesian coordinate system and U, V indicating the non dimensional

coordinate system. If u and v are two parameters, p and q are degree of curves, $(n+1)$ and $(m+1)$ are number of points along U and V direction, $w_{i,j}$ indicates the weight of points $P_{i,j}$, a equation for NURBS surface can also be derived from the extension of equation 2.1.

$$S(t_k, r_l) = \frac{\sum_{i=0}^{n}\sum_{j=0}^{m} N_{i,p}(t_k)N_{j,q}(r_l)w_{i,j}P_{i,j}}{\sum_{i=0}^{n}\sum_{j=0}^{m} N_{i,p}(t_k)N_{j,q}(r_l)w_{i,j}} \tag{2.7}$$

In equation 2.7, $S(t_k, r_l)$ indicates the surface points, t_k and r_l represent parameters on U and V directions. The values of k and l are equal to the number of parameters on U and V direction respectively. Once the surface points are obtained, an input file can be made based on the requirements of the resistance program. To represent the surface of a ship more than one surface patch (segment) may be required. In figure 2.4, the black lines are indicating the border of multiple patches in a ship. After generating surface points from multiple patches the points are joined together to generate a single point field for the ship.

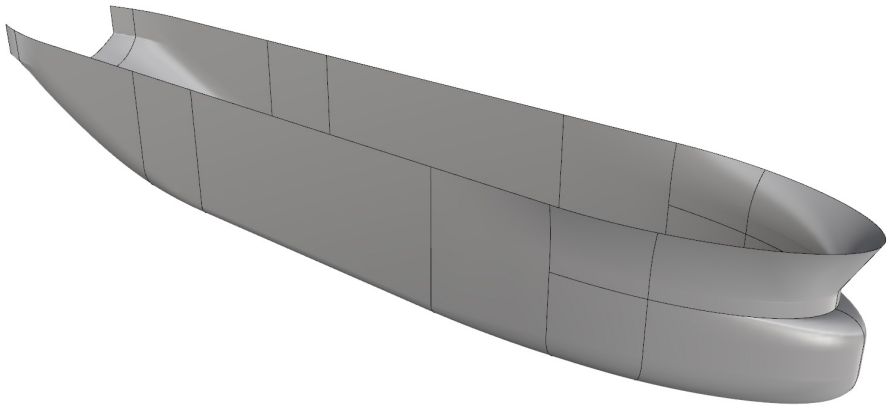

Figure 2.4: Ship with multiple patches

2.2 Developing Kriging Model

2.2.1 Sampling

Surrogate based optimization starts from selecting a suitable set of design variables combination and corresponding responses. For this reason a well organized distribution of variables is required to mimic the whole scenario of the experimental system. Latin hypercube design(LHD) is a statistical model for generating a set of variables combination from multidimensional distribution that fulfil the requirement of representing the whole scenario. It was first described by McKay(Mckay et al. (1979)) in 1979 though a similar technique was also introduced by Eglājs in 1977. The concept behind this design is that there will be one sample point in each sample level. Based on the distribution of points, LHD has different types of designs. In this work a Latin Hypercube Design is used where the sampling points are taken based on random sampling.

2.2.2 Kriging

Kriging is a linear spatial estimation procedure for finding the response of an unknown location from a given sets of points by computing a weighted average of those known values. In figure 2.5, the red point indicating the unknown point where the response is required. Based on responses of the surrounding black points Kriging predict the response on red point. Kriging is based on the assumption of covariance and generally produces a linear unbiased estimator to predict the unknown value. Kriging starts with a set of known values for the neighbouring points of the target points. Each value associated with a spatial location. A new value can be predicted at any new spatial location by calculating the weights on corresponding points. For predicting the response of an unknown point s_0, if the number of neighbouring known locations

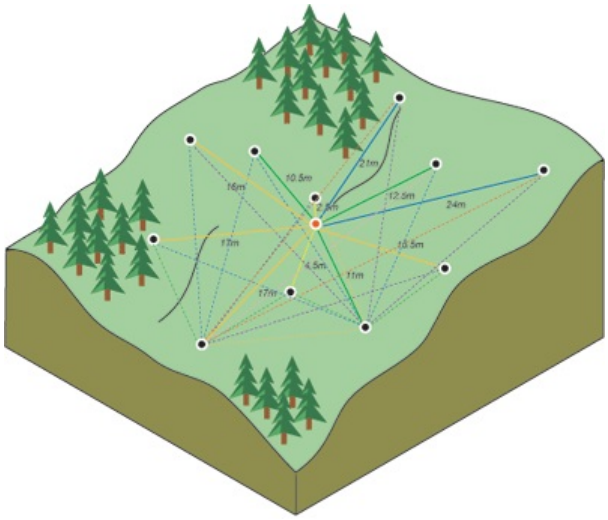

Figure 2.5: Concept of Kriging(http://desktop.arcgis.com)

are n, positions and the responses of those points are respectively (s_1, s_2, s_3,...,s_n) and ($Y(s_1)$,$Y(s_2)$,$Y(s_3)$, ..., $Y(s_n)$), the predicted response $Y(s_0)$ can be defined as follows (Isaaks and Srivastava (1989)).

$$\hat{Y}(s_0) = \sum_{i=1}^{n} w_i Y(s_i) \tag{2.8}$$

where, w_i indicate the weights of points and can be represented as w_i=[w_1, w_2, w_3,...,w_n]. The error($\in_k$) between the predicted and the actual value at any location i can be represented by equation 2.9.

$$\in_{ki} = \hat{Y}(s_i) - Y(s_i) \tag{2.9}$$

For any point s_0, the expected error can be written by

$$E(\in_{k0}) = E\left(\hat{Y}(s_0) - Y(s_0)\right) \tag{2.10}$$

The expected value for each response will be same as it is considered that each of point has same probability of giving expected value. From this point of view equation 2.11 can be written.

$$E(Y(s_1)) = E(Y(s_2)) = ... = E(Y(s_n)) = E(Y(s_0)) = E(Y) \tag{2.11}$$

If we set the expected error to be zero, it is possible to get an unbiased prediction for point s_0. From this consideration a condition is derived.

$$\begin{aligned} 0 &= E(\in (s_0)) \\ &= E\left(\hat{Y}(s_0)\right) - E\left(Y(s_0)\right) \\ &= E\left(\sum_{i=1}^{n} w_i Y(s_i)\right) - E\left(Y(s_i)\right) \\ &= \sum_{i=1}^{n} w_i E(Y) - E(Y) \\ &= E(Y)(\sum_{i=1}^{n} w_i - 1) \end{aligned} \tag{2.12}$$

or,

$$\sum_{i=1}^{n} w_i = 1 \tag{2.13}$$

The variance of the error from the Kriging can be expressed as σ^2 and it can be described in form of matrices (Sakata et al. (2004)).

$$\sigma^2(s_0) = -\mathbf{w}^T \Gamma \mathbf{w} + 2\mathbf{w}^T \gamma^* \tag{2.14}$$

where, $\mathbf{w}=\{w_1, w_2, ..., w_n\}^T$, $\gamma^*=\{\gamma(s_1 - s_0),\ \gamma(s_2 - s_0),\gamma(s_3 - s_0),...,\gamma(s_n - s_0)\}^T$ and $\Gamma=\{\gamma(s_i - s_j)\}_{ij}$. $\gamma(s_i - s_j)$ indicates corelational function between s_i and s_j. This is also known as semivariogram. To get accurate prediction from Kriging, it

is required to minimize the variance of error. A Lagrangian function ϕ_L can be introduced based on the condition of unbiasedness.

$$\phi(w,\lambda)_L = -\mathbf{w}^T\Gamma\mathbf{w} + 2\mathbf{w}^T\gamma^* - 2\lambda(\mathbf{w}^T 1 - \mathbf{1}) \tag{2.15}$$

where λ is the Lagrange multiplier and $\mathbf{1}$ $=(1,1,1,...,1)^T$. Based on the stationary condition, $\delta\phi_L = 0$ we can get the following equation,

$$\begin{pmatrix} \gamma^* \\ 1 \end{pmatrix} = \begin{pmatrix} \Gamma & \mathbf{1} \\ \mathbf{1^T} & 0 \end{pmatrix} \begin{pmatrix} w \\ \lambda \end{pmatrix} \tag{2.16}$$

By solving the equation of the above expression, the value for the weights can be determined. By plugging the value of $\mathbf{w}$ in equation 2.8, the predicted values can be calculated.

In Kriging process, semivariogram models are used for constructing the coefficient matrix Γ. There are several acceptable models that can be used to meet the purpose such as spherical model, exponential model, gaussian model, power model etc. A set of standard semivariogram models are introduced here (Bailey and Gatrell (1995)) from equations 2.17 to 2.21. For all the described models $\gamma(h)$ is the semivariance for interval distance h, c_0 is the nugget value ($c_0 \geq 0$), a is the lag value and c_1 is a constant value($c_1 \geq 0$).

Spherical model: The spherical model is one of the most commonly used models. This model exhibits good result if the spatial correlation between points decreases approximately linearly with the separation distance and after certain limit it becomes zero.

$$\gamma(h_{ij} = \begin{cases} c_0 + c_1(1.5\frac{h}{a}) - 0.5(\frac{h}{a})^3), & \text{if } h \leq a \\ c_0 + c_1, & \text{otherwise} \end{cases}, \tag{2.17}$$

Gaussian model: Like the spherical model this model is also very popular. This model is used when the correlation between nearest points are very strong and after a certain distance the relation become very minimal.

$$\gamma(h) = \begin{cases} c_0 + c_1\left[1 - exp\left(- (\frac{|h|}{a})^2\right)\right], & \text{if } h \neq 0 \\ 0, & \text{if } h = 0 \end{cases}, \tag{2.18}$$

Exponential Model: This model is similar like spherical but it reaches the sill almost asymptotically.

$$\gamma(h) = \begin{cases} c_0 + c_1\left[1 - exp\left(- 3(\frac{|h|}{a})\right)\right], & \text{if } h \neq 0 \\ 0, & \text{if } h = 0 \end{cases}, \tag{2.19}$$

Linear Model: This model never reaches the sill. Based on the gradient of the line it indicates that how the points are related based on the distance of points.

$$\gamma(h) = \begin{cases} c_0 + c_1|h|, & \text{if } h \neq 0 \\ 0, & \text{if } h = 0 \end{cases}, \tag{2.20}$$

Power Model: This model also does not reach the sill. This model is similar like linear model except the non linearity. Generally linear and power models are points

have long range correlation.

$$\gamma(h) = \begin{cases} c_0 + c_1 h^{c_2}, & \text{if } h \neq 0 \\ 0, & \text{if } h = 0 \end{cases}, \tag{2.21}$$

where, $0<c_2<2$.

2.3 Optimization

2.3.1 Path of Steepest Descent (PSD)

Path of steepest descent is a very popular method to find the optimized results from a problem because of its ease of use and simplicity. The whole procedure of PSD can be subdivided into three sections: screening response, steeping ascent or descent and model for optimization. In screening the response step, initially a factorial design is generated. Based on the outcome of the design a first order equation is made by ignoring the nonlinear effect. If the number of variables is k and the level of run is 2, the total number of run will be 2^k. By considering n as the number of run and y as the outcome of each run, the first order equation can be written as follows (Borkowski (2016)),

$$y = b_0 + \sum_{i=1}^{k} b_i x_i \tag{2.22}$$

where, y = the estimated value, x_0, x_1, x_2,..., x_k = variables and b_0, b_1, b_2,..., b_k = regression coefficients. Based on the outcome of the full factorial design and considering no random error, equation (2.22) can be written as follows.

$$Y = Xb \tag{2.23}$$

where the Y, X and b can be defined as

$$Y = \begin{pmatrix} y_1 \\ y_2 \\ \vdots \\ y_n \end{pmatrix}, X = \begin{pmatrix} 1 & x_{1,1} & x_{1,2} & \cdots & x_{1,k} \\ 1 & x_{2,1} & x_{2,2} & \cdots & x_{2,k} \\ \vdots & \vdots & \vdots & \ddots & \vdots \\ 1 & x_{n,1} & x_{n,2} & \cdots & x_{n,k} \end{pmatrix}, b = \begin{pmatrix} b_0 \\ b_1 \\ \vdots \\ b_k \end{pmatrix} \tag{2.24}$$

Equation 2.23 can be solved for regression coefficients by simple transformation of the matrix X,

$$b = (X^T X)^{-1} X^T Y \tag{2.25}$$

where X^T indicates the transpose of matrix X. After generating the equation, the model moves forward by changing the magnitude of variables by a step length of l_i. The values of l_i can be defined by equation 2.26 (NIST (2016)).

$$l_i = \frac{\triangle b_i}{\sqrt{\sum_{i=1}^{k} b_i^2}} \tag{2.26}$$

where, k indicates number of variables, $\triangle$ represents a value that is controlled by step length. The model keeps moving on the direction of steepest ascent (or descent, as required) until there is no further improvement in the response. Once the model finds no other improvement on the search path, a new factorial experiment with center runs is conducted to determine a new search direction. This process is repeated until a significant curvature is achieved on the path. Figure 2.6 shows the behaviour of line search along steepest ascent or descent. To understand the behaviour of curvature, a model like central composite designs (CCD), Box-Behnken design (BBD) etc. can be introduced. In this work a second order equation is created by using CCD (figure 2.7). The second order model includes linear terms, cross product terms and a second

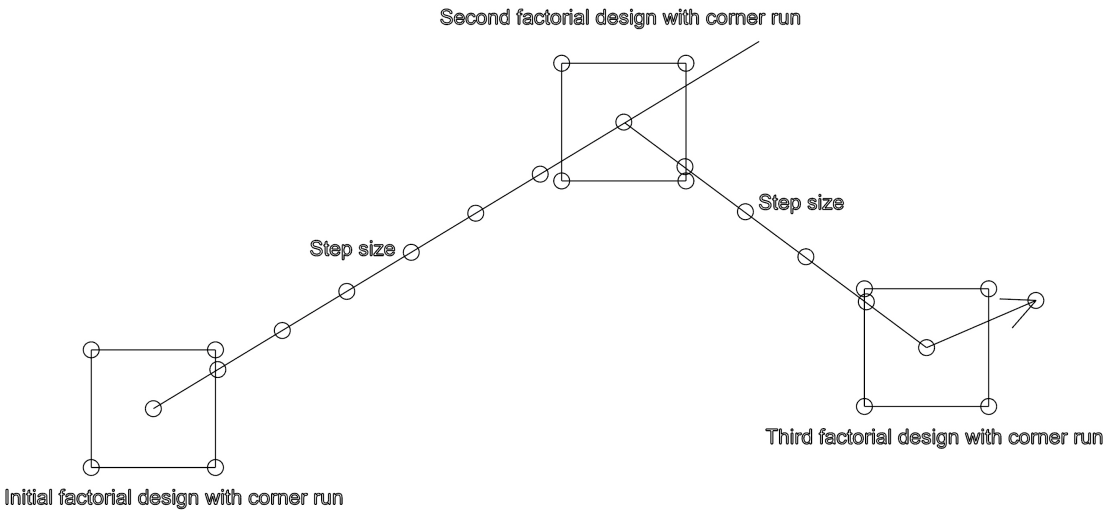

Figure 2.6: Sequence of steepest path search for two factors optimization

order term for each variable. Then equation for second order regression model can be written as follows.

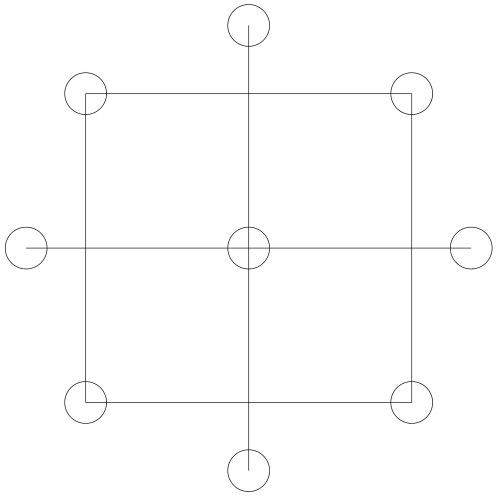

Figure 2.7: Central composite designs for the optimization of two variables

$$y = b_0 + \sum_{i=1}^{k} b_i x_i + \sum_{i=1}^{k} b_{ii} x_i^2 + \sum_{i<j}^{k} b_{ij} x_i x_j \tag{2.27}$$

where, $b_i = b_1, b_2, b_3, ..., b_k$, $b_{ij} = b_{12}, b_{23}, ...$ and $b_{ii} = b_{11}, b_{22}, b_{33}, ..., b_{kk}$. From the second order regression equation the maximum, minimum or saddle point(x_m)

can be represented by equation 2.28.

$$x_m = -\frac{1}{2}B^{-1}b \tag{2.28}$$

where as B^{-1} is the inverse matrix of B. B and b can be written as,

$$x_m = \begin{pmatrix} x_1 \\ x_2 \\ \vdots \\ x_k \end{pmatrix}, B = \begin{pmatrix} b_{1,1} & \frac{b_{1,2}}{2} & \cdots & \frac{b_{1,k}}{2} \\ \frac{b_{2,1}}{2} & b_{2,2} & \cdots & \vdots \\ \vdots & \vdots & \ddots & \vdots \\ sym & \cdots & \cdots & b_{k,k} \end{pmatrix}, b = \begin{pmatrix} b_1 \\ b_2 \\ \vdots \\ b_k \end{pmatrix} \tag{2.29}$$

After that by using x_m the optimized value can be achieved.

2.3.2 Broyden Fletcher Goldfarb Shanno algorithm

Multivariable search methods use a sequential search method that terminates when a convergence test is satisfied. Different multivarible optimization algorithms, like gradient method, Newton's method, Quasi-Newton method, DFP use different types of search method. In sequential multivariable search methods calculating gradient and Hessian matrix play the key role. Based on the search procedure the duration of optimization procedure varies.

In DFP method the calculation of the Hessian matrix is required but quasi-Newton method does not calculate the Hessian matrix for the search method. In the gradient search method the gradient plays the key role for searching the optimal value whereas Newton's method uses the inverse of the Hessian matrix. The major difference between BFGS and DFP is that the Hessian matrix is updated iteratively in BFGS method wheras DFP method uses the inverse of Hessian matrix. The Broyden Fletcher Goldfarb Shanno algorithm (BFGS) is the modified procedure of quasi-newton method.

This procedure uses quadratic Taylor approximation of the objective function in variables search direction. One of the main benefits of this method is that it gives good results in solving the non-smooth problems. In this algorithm the whole system moves forward by calculating the inverse Hessian matrix. The procedure can be described by the following steps (Rao (1996)).

1. BFGS algorithm starts by calculating directional matrix, P_k from equation (2.30) where $\nabla f(x_k)$ and $[B_k]$ are the derivative of $f(x_k)$ and initial Hessian matrix respectively. The initial Hessian matrix $[B_1]$ is assumed to be equal to unity matrix I.

$$P_k = -[B_k]\nabla f(x_k) \tag{2.30}$$

2. Later on the calculated P_k is used for line search where an acceptable method (Wolfe conditions, Fibonacci method, etc) require for obtaining a step length α_k that ensure sufficient change is the value of function. The process of calculating new values for the variables can be defined as follows,

$$x_{k+1} = x_k + \alpha_k P_k \tag{2.31}$$

3. Once the value of α_k is being calculated, a new parameter s_k is measured from the step length and directional matrix by equation (2.32) .

$$s_k = \alpha_k P_k \tag{2.32}$$

4. Later on the difference between consecutive gradient y_k and consecutive value d_k are calculated.

$$y_k = \nabla f(x_{k+1}) - \nabla f(x_k) \tag{2.33}$$

$$d_k = x_{k+1} - x_k \tag{2.34}$$

5. The successive Hessian matrix can be calculated by the following equation

$$[B_{k+1}] = [B_k] + \left(1 + \frac{y_k^T [B_k] y_k}{d_i^T y_k}\right) \frac{d_k d_k^T}{d_k^T y_k} - \frac{d_k y_k^T [B_k]}{d_k^T y_k} - \frac{[B_k] y_k d_k^T}{d_k^T y_k} \tag{2.35}$$

After this step the algorithm goto step 2 and continue till get a optimized result. For line search a popular inexact line search condition is used in this thesis that gives sufficient decrease in the objective function $f(x)$ as measured by the following inequalities.

$$f(x_k + \alpha_k P_k) \leq f(x_k) + a_1 \alpha_k P_k^T \nabla f(x_k) \tag{2.36}$$

$$P_k^T \nabla f(x_k + \alpha_k P_k) \geq a_2 P_k^T f(x_k) \tag{2.37}$$

where the values of a_1 and a_2 can be represented as $0 < a_1 < a_2 < 1$. In generally a_1 is considered to be a very small value, say $a_1 = 10^{-4}$. Equation (2.36) and (2.37) are known as the Armijo rule (Armijo (1966)) and curvature condition respectively . Based on Wolfe conditions, the step length of a function is calculated for which the value of function varies significantly. In some cases wolfe conditions can not calculate the step length α to ensure the progress toward the extreme value of a function. To solve this problem some modification is introduced on equation (2.37) that ensure to find proper step length α.

$$\left| p_k^T \nabla f(x_k + \alpha_k p_k) \right| \leq \left| a_2 p_k^T f(x_k) \right| \tag{2.38}$$

Together equation (2.36) and (2.38) known as the stronge Wolfe conditions.

2.4 Wave Making Resistance

In this thesis the optimization is carried out on the basis of wave making resistance of ship. A wave making resistance program MAPS-Resistance is being used here. The theoretical background of MAPS wave making resistance calculation can be described as follows (Peng et al. (2014)).

2.4.1 MAPS-Resistance

Consider a surface ship is travelling with steady forward speed U in calm water, a ship-fixed Cartesian coordinate system xyz is employed with the positive z-axis upwards and the positive x-axis pointing from the bow to the stern. The origin is set on the undisturbed water surface intersecting with the midship section and the centre plane. After using velocity potential on Laplace equation, the expression can be described as follows,

$$\bigtriangledown^2\phi = 0 \tag{2.39}$$

If Φ is the velocity potential of the basic flow of a body translating in an infinite fluid and φ is the disturbed velocity potential, the total velocity potential can be expressed as,

$$\phi = \Phi + \varphi \tag{2.40}$$

The body boundary condition on the wetted surface of the ship hull is

$$\frac{\partial\phi}{\partial n} = 0 \tag{2.41}$$

where the outward normal vector from the ship hull is denoted by $\overrightarrow{n}$=(n_x, n_y, n_z). The kinematic free surface condition and dynamic free surface condition can be expressed

as equation 2.42 and 2.43 respectively.

$$\eta_x\phi_x + \eta_y\phi_y - \phi_z = 0 \quad on \quad z = \eta(x, y) \tag{2.42}$$

$$\eta = \frac{1}{2g}(U_0^2 - |\nabla\phi|^2) \quad on \quad z = \eta(x, y) \tag{2.43}$$

where η is the free surface elevation and the subscripts denote the partial derivatives on that direction, g is the gravitational acceleration and $\nabla\phi$=(ϕ_x, ϕ_y, ϕ_z). The combined nonlinear free surface condition is then given as

$$\frac{1}{2}\phi_x(\phi_x^2 + \phi_y^2 + \phi_z^2)_x + \frac{1}{2}\phi_y(\phi_x^2 + \phi_y^2 + \phi_z^2)_y + g\phi_z = 0 \quad on \quad z = \eta(x, y) \tag{2.44}$$

After the velocity potential ϕ is solved, the wave elevation on the free surface can be obtained.If the resistance of ship hull is denoted R_w, the resistance can be expressed as follows,

$$R_w = \int_{S_B} \left(1 - \frac{|\nabla\phi|^2}{U^2}\right) n_x dx \tag{2.45}$$

The wave resistance coefficient,C_w, is defined as:

$$C_w = \frac{R_w}{\frac{1}{2}\rho U_0^2 S} \tag{2.46}$$

where, R_w is the wave making resistance, U_0 is forward speed , ρ is water density and S wetted surface area.

Chapter 3

Numerical Method

3.1 Input Generation for MAPS

The wave making resistance calculation program, MAPS resistance has its own geometry input format. A sample input for MAPS resistance is provided on the appendix B. MAPS can handle multiple vertically placed surface patches for calculation. The input of the optimization procedure in this work is an IGES file. An IGES file may have multiple patches. For the sake of necessity in this thesis, all the surface points generated from multiple patches are unified into a single point field. Later on, the point field is arranged in the proper way to make an input file for MAPS resistance.

3.1.1 Unification of multiple patch surface points

In this work, two point distribution methods are introduced to get systemically distributed surface points of the ship.

3.1.1.1 Method 1

For multiple patches in an IGES file, it is common to have patches with different numbers of points. The first method starts with generating a large number of points along V direction of each patch. By using the generated points the arc length of each station is calculated. Once the arc length is known, surface points at suitable distances can be selected from the generated large number of surface points based on the distance from the initial point within a tolerance limit. Once surface points of different patches are distributed similarly along V direction, the surfaces can be merged into a new surface. In figure3.1a, two patches with misaligned surface points are shown. In figure 3.1b, the generation of a large number of surface points by NURBS is illustrated. Figure 3.1c and figure 3.1d indicate aligning and joining the multiple patches to make a single surface point cloud.

3.1.1.2 Method 2

The method 2 is a modified method of Hsiao′s surface grid generation method (Hsiao (1996)). In this method, the arc length for surface along U and V direction are described by $\phi_{i,j}$ and $\psi_{i,j}$ respectively. The definition of $\phi_{i,j}$ and $\psi_{i,j}$ can be described as

$$\phi_{i,j} = \phi_{i,j-1} + \sqrt{[(x_{i,j} - x_{i,j-1})^2 + (y_{i,j} - y_{i,j-1})^2 + (z_{i,j} - z_{i,j-1})^2]} \tag{3.1}$$

$$\psi_{i,j} = \psi_{i-1,j} + \sqrt{[(x_{i,j} - x_{i-1,j})^2 + (y_{i,j} - y_{i-1,j})^2 + (z_{i,j} - z_{i-1,j})^2]} \tag{3.2}$$

where, i and j indicate the serial of the surface point along U and V directions; $x_{i,j}$, $y_{i,j}$and $z_{i,j}$ are the surface points on each patch. The normalized arc length for surface along U and V direction are described by $\phi'_{i,j}$ and $\psi'_{i,j}$ respectively. It can be considered that $\phi'_{1,j}$=$\psi'_{i,1} = 0$ and $\phi'_{imax,j} = \psi'_{i,jmax}$ =1 . For other points the following

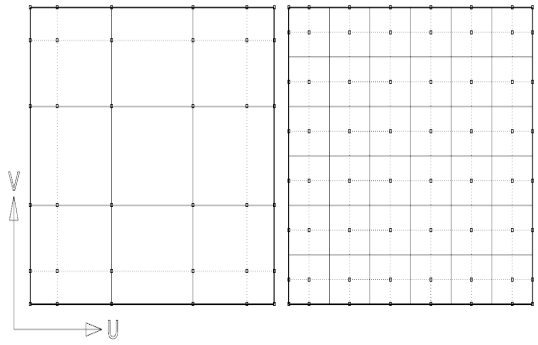

(a) Misaligned surface points on two patches

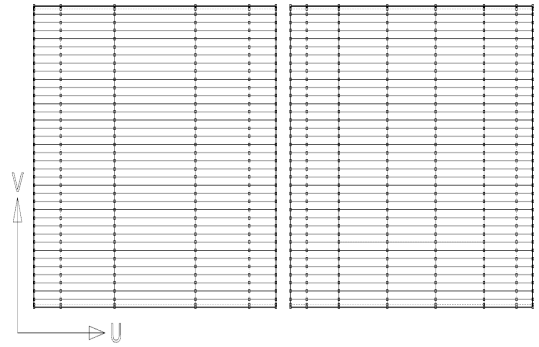

(b) Large number of surface points generation

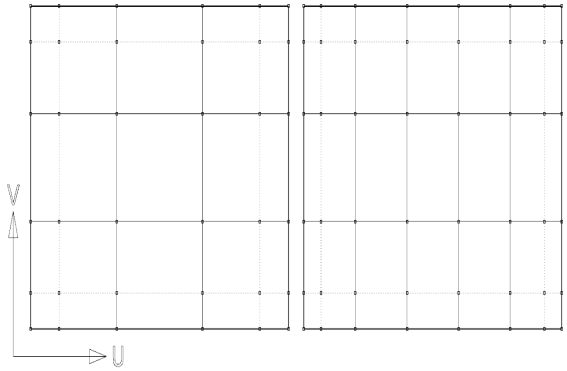

(c) Properly aligned surface points on two patches

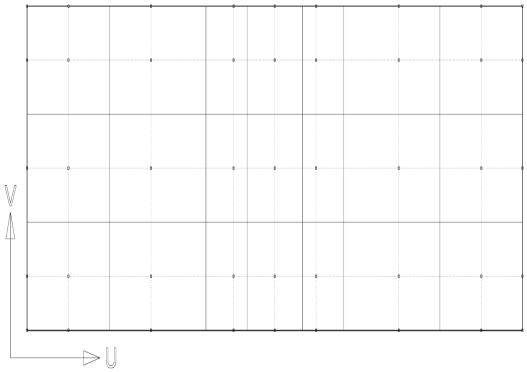

(d) Unification of surface points from two patches

Figure 3.1: Unification of surface points from multiple patches

equation can be used,

$$\phi'_{i,j} = \frac{\phi_{i,j}}{\phi_{imax,j}}, \psi'_{i,j} = \frac{\psi_{i,j}}{\psi_{imax,j}} \tag{3.3}$$

where, $i = 2, 3, ..., (m-1)$ and $j = 2, 3, 4, ..., (n-1)$. By using the normalized arc length the surface points can be written as

$$\begin{aligned} S_x &= \{x_{i,j}, \phi'_{i,j}, \psi'_{i,j}\} \\ S_y &= \{y_{i,j}, \phi'_{i,j}, \psi'_{i,j}\} \\ S_z &= \{z_{i,j}, \phi'_{i,j}, \psi'_{i,j}\} \end{aligned} \tag{3.4}$$

Based on $\phi^{'}$ and $\psi^{'}$, calculation of bi-cubic interpolation is carried out along U and V direction. By using bi-cubic interpolation the surface point rearrangement takes place with the help of ξ and η that depend on the total number of points on U and V directions. If the number of points along U and V directions are N_U and N_V respectively, the value of two parameter ξ and η can be obtained from equation 3.5.

$$\begin{aligned} \xi_i &= \frac{(i-1)}{N_U - 1} \\ \eta_j &= \frac{(j-1)}{N_V - 1} \end{aligned} \tag{3.5}$$

Once the values of ξ and η are achieved, the value of ϕ and ψ can be redistributed by equation 3.6 and equation 3.7.

$$\phi_i^{'} = \frac{1 - a + (a+1)[\frac{a+1}{a-1}]^{2(\xi_i - \frac{1}{2})}}{2 + 2[\frac{a+1}{a-1}]^{2(\xi_i - \frac{1}{2})}} \tag{3.6}$$

$$\psi_j^{'} = \frac{1 + b - (b-1)[\frac{b+1}{b-1}]^{(1-\eta_j)}}{1 + [\frac{b+1}{b-1}]^{(1-\eta_j)}} \tag{3.7}$$

where, a and b indicate two positive real numbers, $a > 1$ and $b > 1$. The distribution of surface points over the surface greatly depends on the value of a and b. If the value of a and b are close to unity, equation 3.6 makes the point distribution denser on both corners of the surface where equation 3.7distribute the points densely on one corner of the surface. If the value of a and b are higher, both equations give approximately equally spaced distributed points. Figure 3.2 gives an idea about different types of points distribution. The main benefit of this method is that it is fast as it does not need to generate large number of points like the method 1.

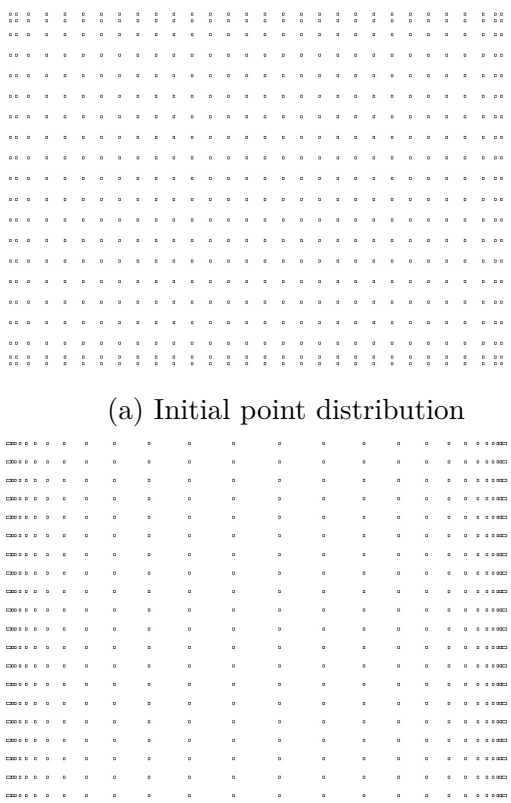

(a) Initial point distribution

(b) Equally spaced point distribution

(c) Points clustered on two opposite corners

(d) Points clustered on a single corner

Figure 3.2: Different types of point distributions

By using this method similar kinds of point distribution can be obtained for multiple patches in an IGES file. Later on the patches can be merged into a single surface point cloud.

3.2 Input for Resistance Calculation

Once a surface point cloud is generated, it is required to distribute the surface points to prepare an input file for MAPS resistance. For calculating the wave making resistance it is important to have denser point distribution on the bow and stern of the ship surface to measure the change of pressure gradient properly. To fulfil the requirement again Hsiao's algorithm is used. In figure 3.3, the steps of input file generation

is shown. Figure 3.3a depicts the graphical representation of a ship with multiple patches. From there, surface points are generated by NURBS (figure 3.3b). Later on points are redistributed and multiple patch distributed surface points are joined together (figure 3.3c). Finally unified surface point cloud is redistributed to make an input for MAPS resistance (figure 3.3d).

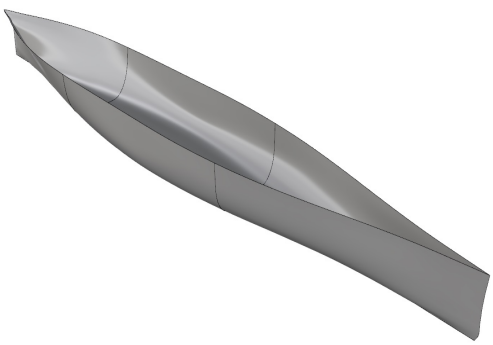

(a) Hull with multiple patches

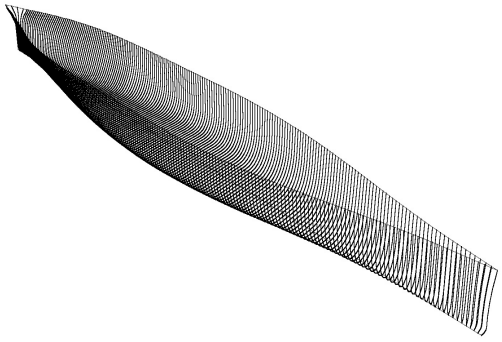

(b) Surface Points from patches

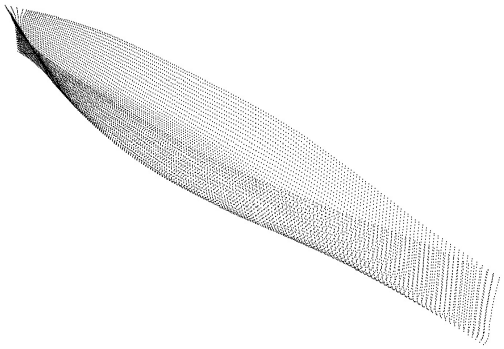

(c) Unified surface points from multiple patches

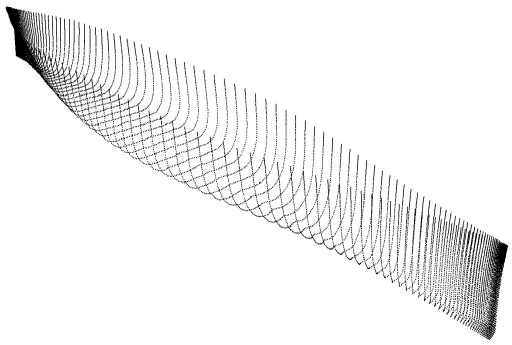

(d) Modified points distribution suitable for calculation

Figure 3.3: Generation of input file for resistance calculation

3.3 Hull Variation

To optimize the ship hull, it is required to modify the ship geometry. There are different ways of modifying the geometry. In this thesis three different methods are

used. The methods are shifting parametric sections globally (schm:1), shifting ship surface sections regionally (schm:2) and modifying the hull by generating a bulbous bow (schm:3).

3.3.1 Shifting Parametric Section Globally (schm:1)

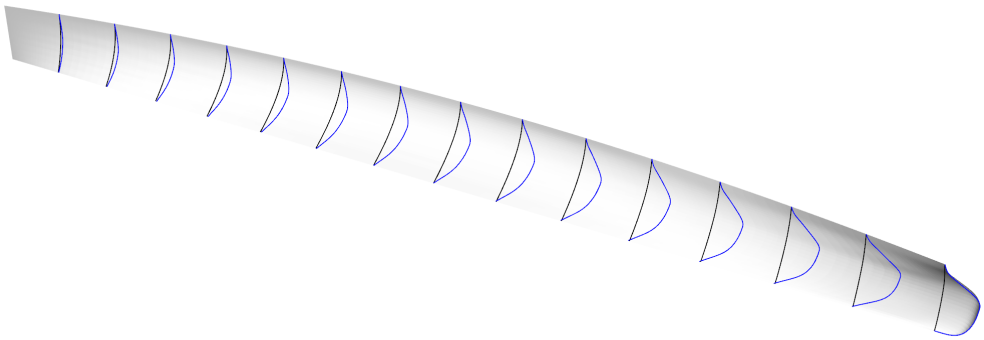

(a) Perspective view of a half ship (blue line = parametric section, black line= real section)

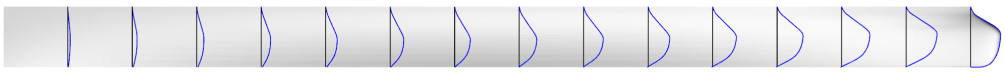

(b) Modified wigley hull

Figure 3.4: (Profile of half ship (blue line = parametric section, black line= real section)

This method is a kind of shifting methods. To understand this method it is required to differentiate between real sections and parametric sections of the ship. In figure 3.4, the difference between real and parametric sections are illustrated. Real sections are perpendicular to the load waterline and generally all the points on a particular real section will have the same x directional coordinate. The parametric sections are generated based on the point distribution on the ship's surface. A set of parametric sections can easily describe a ship easily. In this modification method, the parametric

sections are grouped into two parts, forward part and aft part. The forward part indicates all the parametric sections starting from bow to half of the total number of parametric sections. The aft part represent all the parametric sections from stern of the ship to half of the total number of parametric sections. Later on these two parts are moved along the length of the ship to modify the ship geometry. We can consider x directional surface points of forward part and aft part are $Sxf_{(i,j)}$ and $Sxa_{(i,j)}$ respectively. The number of surface points on U direction are N_V and V direction are N_U. The difference between two consecutive x- directional surface points are $\Delta_{f(i,j)}$ and $\Delta_{a(i,j)}$.

$$\Delta_{r(i,j)} =\mid X_{i,j} - X_{i,j+1} \mid, \text{ where } 1 \leqslant i \leqslant N_U \text{ and } 1 \leqslant j \leqslant (N_V - 1) \tag{3.8}$$

$$\Delta_{l(i,j)} =\mid X_{i,j} - X_{i,j-1} \mid, \text{ where } 1 \leqslant i \leqslant N_U \text{ and } 2 \leqslant j \leqslant N_V \tag{3.9}$$

For each x- directional point from $1 \leqslant i \leqslant N_U$ to $2 \leqslant j \leqslant (N_V - 1)$ there will be two distances namely $\Delta_{r(i,j)}$ and $\Delta_{l(i,j)}$. From there the minimum distances $\delta_{a(i,j)}$ and $\delta_{f(i,j)}$ can be determined.

$$\delta_{a(i,j)} = min\left(\Delta_{r(i,j)}, \Delta_{l(i,j)}\right) \quad \begin{cases} \text{if } N_V \text{ even, } 1 \leqslant i \leqslant N_U \text{ and } 2 \leqslant j \leqslant \dfrac{N_V}{2} \\ \text{if } N_V \text{ odd, } 1 \leqslant i \leqslant N_U \text{ and } 2 \leqslant j \leqslant \dfrac{N_V - 1}{2} \end{cases} \tag{3.10}$$

$$\delta_{f(i,j)} = min\left(\Delta_{r(i,j)}, \Delta_{l(i,j)}\right) \quad \begin{cases} \text{if } N_V \text{ even, } 1 \leqslant i \leqslant N_U \text{ and } \dfrac{N_V}{2} + 1 \leqslant j \leqslant N_V - 1 \\ \text{if } N_V \text{ odd, } 1 \leqslant i \leqslant N_U \text{ and } \dfrac{N_V + 1}{2} + 1 \leqslant j \leqslant N_V - 1 \end{cases} \tag{3.11}$$

Once the minimum distance is known, two coefficients w_f and w_a can be used to

define the amount of deformation of $Sf_{(i,j)}$ and $Sa_{(i,j)}$.

$$Sf_{(i,j)} = w_f \delta_{f(i,j)} \tag{3.12}$$

$$Sa_{(i,j)} = w_a \delta_{a(i,j)} \tag{3.13}$$

Then based on the amount of deformation the new position of $Sxf_{(i,j)}$ and $Sxa_{(i,j)}$ can be written as follows,

$$Snf_{(i,j)} = Sxf_{(i,j)} + v_1 Sf_{(i,j)} \tag{3.14}$$

$$Sna_{(i,j)} = Sxa_{(i,j)} + v_2 Sa_{(i,j)} \tag{3.15}$$

where, v_1 and v_2 are two parameters those control the amount of shifting. The values of v_1 and v_2 can be between 0 to 1. $Snf_{(i,j)}$ and $Sna_{(i,j)}$ are the new positions of $Sxf_{(i,j)}$ and $Sxa_{(i,j)}$ respectively where $1 < i < N_u$ and $2 < j < (N_v - 1)$. For all $1 < i < N_u$, $Snf_{(i,1)}$=$Sxf_{(i,1)}$ and $Sna_{(i,1)}$=$Sxa_{(i,1)}$. The benefit of this modification technique is that the hull will never be distorted. It will always give realistic ship hull and at the same time the deviation of original ship hull will be minimal. The benefit of using w_f and w_a are that if the values are higher than one still there will be no overlapping except the first and the last column. To get rid of these kind of problems the values of w_f and w_a are better to keep less than one. Figures 3.5, 3.6 and 3.7 depict the procedure of surface point movement based on this technique.

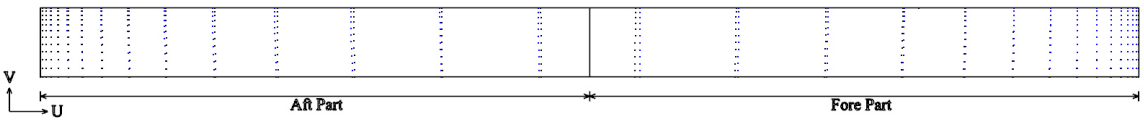

Figure 3.5: Hull with original and modified surface points

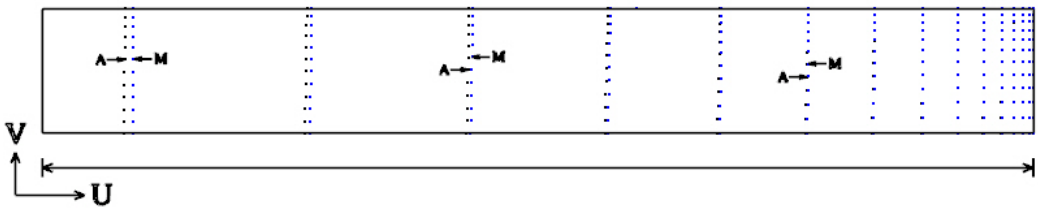

Figure 3.6: Original(A) and Modified(M) forward surface points

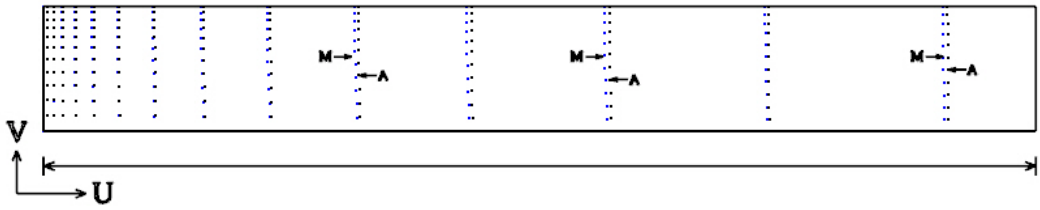

Figure 3.7: Original(A) and Modified(M) aft surface points

3.3.2 Regional Shifting Method (schm:2)

This method is another kind of shifting method which was first introduced by Kim and Yang (2010a). Later on they have done some further related work based on this method (Kim and Yang (2013)). It is a modified technique of Lackenby′s hull variation procedure (Lackenby (1950)). The main benefit of using this technique is that it prevents the generation of the unrealistic hull forms associated with the movement of the new sectional area curve Kim and Yang (2010a). Beside this the initial hull form can be modified without evaluating the initial and modified sectional area curves. At the time of optimization the sectional area curve changes on the basis of two variables.

If the sectional area curve (SAC) of a ship can be defined by S^0 and sectional area curve after modification is $S^{'}$, then the relation between these two curves can be expressed as follows.

$$S^{'} = S^0 + f(x, a_1, a_2) \tag{3.16}$$

where, a_1 indicates a parameter and a_2 refers to the position where the coordinate of ship section will remain fixed.The amount of shifts are defined by a_1. The modification function f can be expressed as follows.

$$f(x, a_1, a_2) = \begin{cases} a_1\Big(0.5(1 - \cos 2\pi \dfrac{x - x_1}{a_2 - x_1})\Big)^{\dfrac{1}{2}} & x_1 \leq x \leq a_2 \\ -a_1\Big(0.5(1 - \cos 2\pi \dfrac{x - a_2}{a_2 - x_2})\Big)^{\dfrac{1}{2}} & a_2 \leq x \leq x_2 \\ 0 \qquad\qquad \text{elsewhere} \end{cases} \tag{3.17}$$

where x_1 and x_2 indicate the starting and finishing positions of the region where the shifting will occur. In the hull modification method, the positions of x_1 and x_2 are kept fixed. Then a_1 and a_2 vary based on the optimization procedure. The main benefit of this procedure is that there is less chance of having abrupt or impractical ship hull generation. In figure 3.8, x_1 and x_2 indicate the range of hull modification. $S(x)$, $S^{'}(x)$ and $f(x)$ indicate the original sectional area curve, modified sectional area curve and modification function respectively.

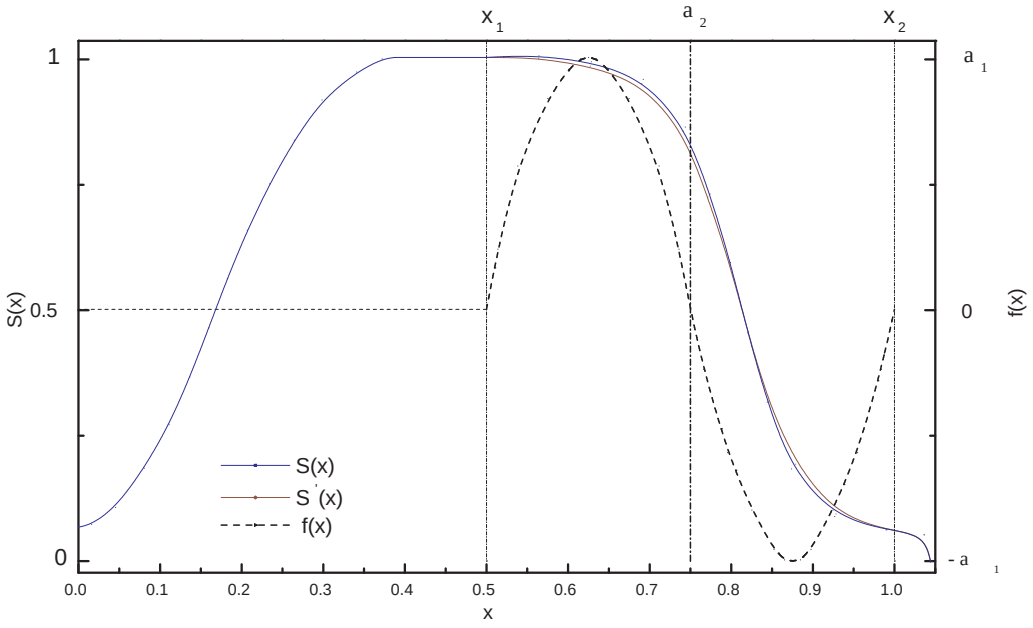

Figure 3.8: Comparison of original and modified sectional area

3.3.3 Generating Bulbous Bow by Modifying the Bow (schm:3)

The concept of using a bulb like shape with the ship hull to reduce the resistance was first introduced by R. E. Froude (Kratch (1978)). Later on D.W. Taylor first recognized the bulbous bow as a part of ship to reduce the wave making resistance of a ship. A bulb can be represented roughly by using a fewer number of parameters. Kratch (1978) divided the bulbs into three types: $\triangle$ type, O type and $\bigtriangledown$ type (figure 3.9). Generally a bulb can be represented by three linear and three nonlinear coefficients. A illustration of bulb can be introduced here to depict the geometry of a bulbous bow (figure 3.10). The parameters of the bulb are L_{PR}= protruding length of the bulb, B_B= bulb breadth at forward perpendicular, Z_B= height of the bulb from keel at maximum L_{PR}, L_{PP}= length between perpendiculars, B= breadth of the midship, T= draft and V= displacement of the ship. Based on these parameters

three linear and three nonlinear coefficients can be described. Based on the detail works on bulbous bow of Kratch (1978), a table is introduced where the maximum and the minimum limit of bulb parameters are provided 3.1, although these values also depend on the block coefficient, prismatic coefficient, volume and other factors of the ship geometry. Beside this in table 3.2, a comparison of these coefficients are provided for different types of ships.

Wigley, Series60, S175 or other this kind of ship can easily be modified by this method. To obtain a bulb like shape, the bow of the ship is modified based on trigonometric functions. Based on the characteristics of $Sin^n(x)$, the profile of the bulbous bow is generated where n is a positive number. The main problem of using $Sin(x)$ function is that though it creates a bulbous shape at the bow, it generates a very narrow bulb. To overcome this problem again the bow part of the waterlines are modified based on a exponential function e^{mx} where m is a positive number.

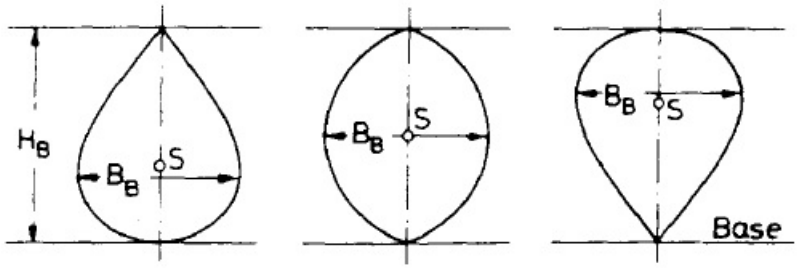

Figure 3.9: Types of bulbous bow $\triangle$ type, O type and $\bigtriangledown$ type(Kratch (1978))

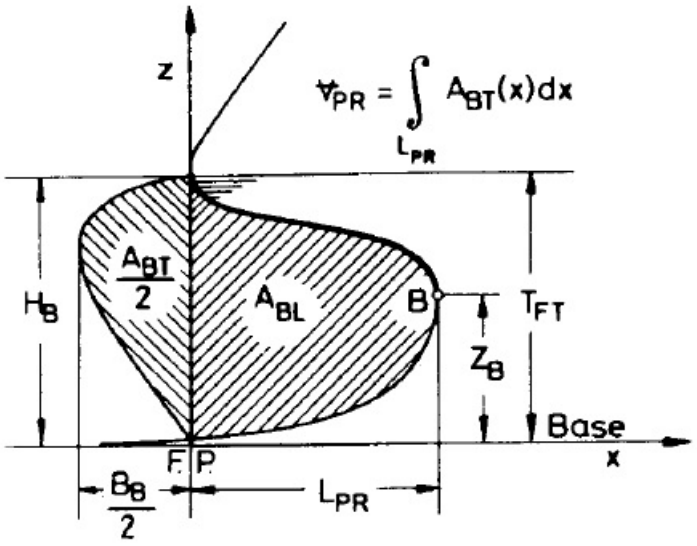

Figure 3.10: Parametrs of bulbous bow (Kratch (1978))

Table 3.1: Typical values of bulb coefficients

Parameters	Symbol	Ratio	Minimun	Maximum
Linear coeff	C_{LPR}	L_{PR}/L	0.0180	0.0310
Breadth coeff	C_{BB}	B_b/B	0.170	0.200
Depth coeff	C_{ZB}	Z_B/T	0.260	0.550
Lateral coeff	C_{ABL}	A_{BL}/A_{Mid}	0.068	0.146
Trans.Area coeff	C_{ABT}	A_{BT}/A_{Mid}	0.064	0.122
Volume coeff	C_{VPR}	V_{PR}/V	0.0011	0.00272

Table 3.2: Range of parameters for bulb geometry for different hulls

Parameters	Symbol	Ratio	KCS container	KVLCC2	S175
Linear coeff	C_{LPR}	L_{PR}/L	0.0297	0.0249	0.009609
Breadth coeff	C_{BB}	B_b/B	0.1500	0.2415	0.0529
Depth coeff	C_{ZB}	Z_B/T	0.5731	0.5096	0.2537
Lateral coeff	C_{ABL}	A_{BL}/A_{Mid}	0.1359	0.07198	0.03914
Trans.Area coeff	C_{ABT}	A_{BT}/A_{Mid}	0.0857	0.1439	0.07828
Volume coeff	C_{VPR}	V_{PR}/V	0.001254	0.002053	0.000164
Block coeff	C_B	V_{PR}/V	0.651	0.8098	0.5859

For better understanding this method can be divided into three parts: changing the bow profile, changing the bulb breadth, generating the bow and smoothing the surface.

3.3.3.1 Changing the Bow Profile

At first the bow of the ship is changed based on the coefficient C_{LPR} and C_{ZB}. These two coefficients indicate the maximum length of bulb (L_{LPR}) and the height of the maximum length from the keel (Z_B). The X directional coordinates of profile can be represented by x_U and x_D where U and D are indicating position of points above the maximum length of bulb and below the maximum length of bulb respectively. d_U and d_D are distances of any point along waterline and keel from the maximum length of bulb respectively (figure 3.11). If $x_U^{'}$ and $x_D^{'}$ are X directional coordinates of modified profile (above and below the maximum length of bulb respectively), these can be obtained by equation 3.18 and 3.19.

$$x_U^{'} = x_U + \Delta x_U = x_U + L_{LR}.\sin^a\{(1 - \frac{d_U}{T - Z_B})\frac{\pi}{2}\} \tag{3.18}$$

$$x_D^{'} = x_D + \Delta x_D = x_D + L_{LR}.\sin^b\{(1 - \frac{d_U}{Z_B})\frac{\pi}{2}\} \tag{3.19}$$

where, a and b are two positive values; Δx_U and Δx_D are the change of lengths of x_U and x_D respectively.

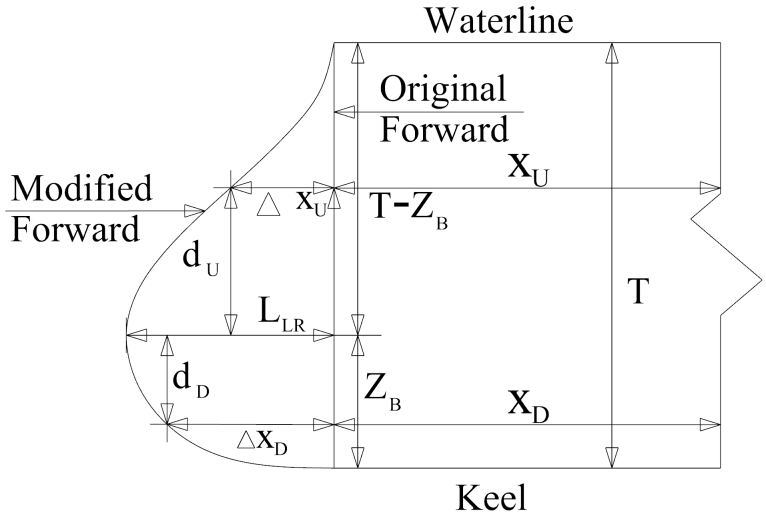

Figure 3.11: Original and modified bow of a hull with parameters

3.3.3.2 Changing the Bulb Breadth

Once the profile of the ship is modified based on L_{PR} and Z_B, the bulb sectional area is required to change based on the value of bulb breadth, B_B. Equation 3.20 and 3.21 are developed based on the value of B_B to generate bulb like sections.

$$y_U = \frac{B_B}{2}.e_U.\sin^c\{(1-\frac{d_U}{T-Z_B})\frac{\pi}{2}\} \tag{3.20}$$

$$y_D = \frac{B_B}{2}.e_D.\sin^d\{(1-\frac{d_D}{Z_B})\frac{\pi}{2}\} \tag{3.21}$$

where, c and d are two positive values; e_U and e_D are two parameters to give steepness to the bulb section respectively. The value of e_U and e_D can be a constant, algebraic, sinusoidal or exponential function. In this work, a sinusoidal function is selected for e_U and a constant for e_D. A typical section of bulb at forward perpendicular is depicted on figure 3.12.

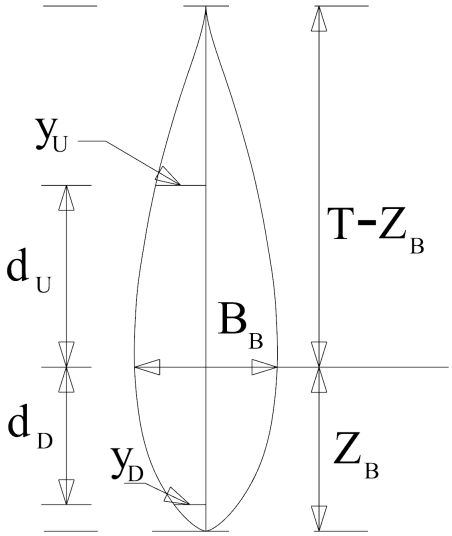

Figure 3.12: Bulb section parameters at forward perpendicular

3.3.3.3 Generating the Bow

After making the profile and sections of the bow, the waterlines at the bow are generated based on the value of y_U and y_D. The breadth at any position on the bulb can be generated by $y_U^{'}$ or $y_D^{'}$.

$$y_D^{'} = y_D.\{1 + \frac{1 - e^{kr_D}}{e^k - 1}\} \tag{3.22}$$

$$y_U^{'} = y_U.\{1 + \frac{1 - e^{kr_U}}{e^k - 1}\} \tag{3.23}$$

On equation 3.22 and 3.23, k indicates a constant value and $0 \leq r_D, r_U \leq 1$. Based on the value of k, the shape of bulb waterlines varies. In figure 3.13, each waterline shows how the waterlines are propagating based on equation 3.22 and 3.23.

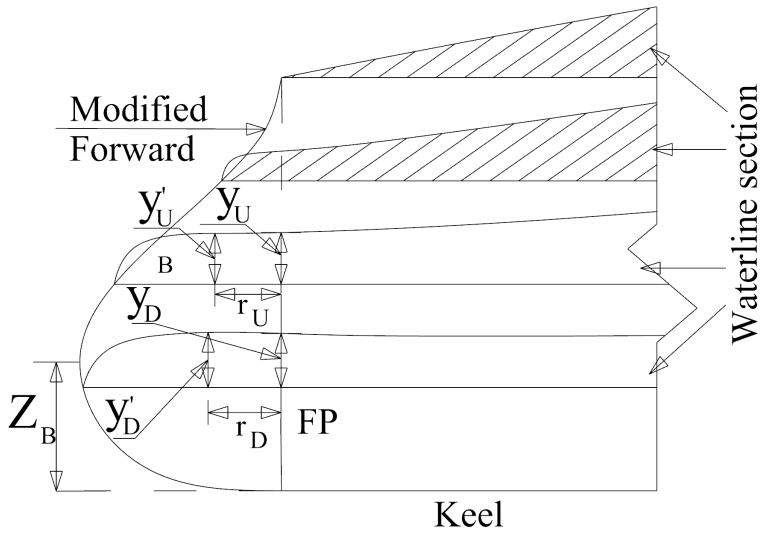

Figure 3.13: Modified waterlines of Wigley(I) hull bow

3.3.3.4 Smoothing the Surface

In this method at the time of bulb sections generation, sometimes the forward hull surface become unsmooth. To avoid this kind of smoothing problem a simple algorithm can be used. There are multiple types of smoothing / filtering methods. In this work two different types of smoothing algorithm are introduced, Gaussian smoothing and Moving mean smoothing.

• Gaussian Smoothing

Gaussian smoothing method is a very widely used method. Taubin (1995) introduced a detail description of this method. If the number of points is n, coordinate of generated point is $x_i^{'}$, coordinate of existing point is x_i, weight is λ whose value can be zero to one, then the modified points for the curve/surface can be written as follows,

$$x_i^{'} = x_i + \lambda \triangle x_i \tag{3.24}$$

Here $\triangle x_i$ indicates the amount of effect of surrounding points. This effect also depends on the value of weight w.

$$\triangle x_i = \frac{1}{2} w \Big[(x_{i-1} - x_i) + (x_{i+1} + x_i) \Big] \tag{3.25}$$

• **Moving Mean Smoothing**

In this method, modified points are generated from a series of averages of different subsets of the full point set. The modified points can be the average of two to higher number of points. As the number of points for obtaining average increases, the modified curve become smoother and shrinker. The effect of smoothing can be demonstrated in figure 3.14 where the right side of the figure is giving a comparison between original hull and hull after gaussian smoothing. On the other side a comparison between original hull and hull after mean smoothing is demonstrated.

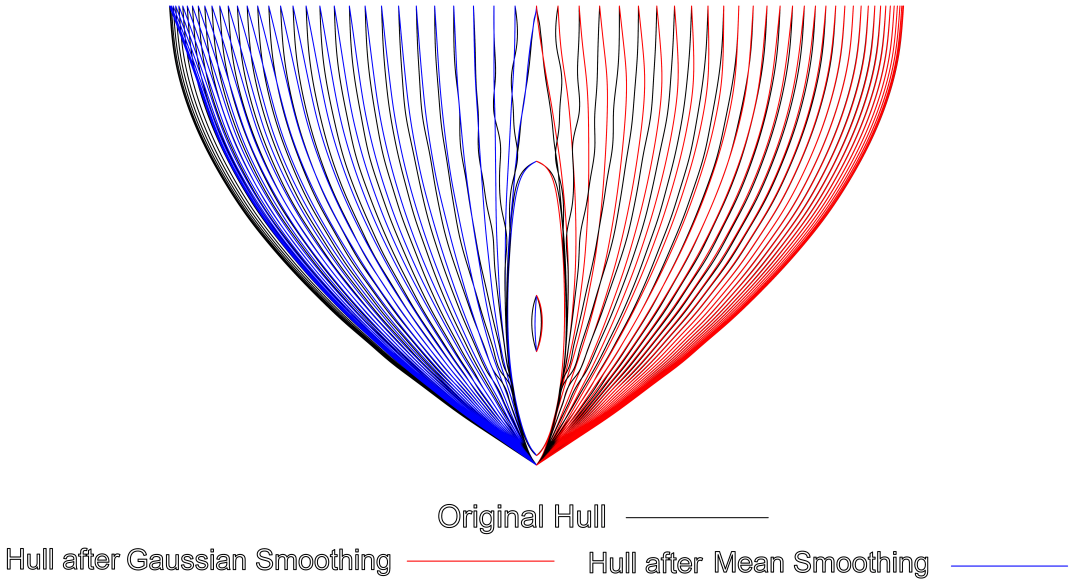

Figure 3.14: Comparison of surface smoothing methods

Chapter 4

Numerical Results

This chapter describes the geometry and wave making resistance of the optimized hulls. Comparisons are also made based on hull properties and wave making resistance of ships. Three different types of hull, Wigley(I), Series 60 and KCS container hulls are investigated to examine the performance of the proposed ship hull optimization technique. The results for different hulls are represented separately for convenience. At first Path of steepest descent (PSD) is used for Wigley(I) and Series 60 hulls. As this method takes huge computational time, Kriging is introduced to predict the wave making resistance of ships. For better result, an updated optimization method Broyden−Fletcher−Goldfarb−Shanno algorithm (BFGS) is used with Kriging method.

4.1 Validation of Optimization Methods

In this thesis two different optimization methods known as PSD and BFGS are introduced for optimization. A fortran program is developed for implementing these two methods. Before using these methods for optimization it is required to validate both of these methods. Two function named as Sphere function (Raska and Ulrych (2014))

and Booth's function (Hedar (2004)) are used to validate the optimization methods. The Sphere function can be defined by equation (4.1) and an illustrative depiction is provided on figure 4.1 for two variables. This function generates it's minimum value 'zero' at point $(0, 0)$.

$$f(x) = \sum_{i=1}^{n} x_i^2 \tag{4.1}$$

The Booth′s function is a non convex function and can be defined by equation (4.2) and can be illustrated by figure 4.2.

$$f(x_1, x_2) = (x_1 + 2x_2 - 7)^2 + (2x_1 + x_2 - 5)^2 \tag{4.2}$$

This function gives minimum value 'zero' at point $(1, 3)$. Within the domain of $-2 \leq x_i \leq 2$ and $-10 \leq x_1 \leq 10$, PSD and BFGS methods are applied to find the optimum points respectively. Table 4.1 provides a comparison between actual minimum value

Table 4.1: Validation of PSD for optimization

	Actual		PSD	
	coordinate	value	coordinate	value
Sphere function	(0,0)	0.00	$(1.13 \times 10^{-5}, -1.99 \times 10^{-3})$	3.99×10^{-6}
Booth function	(1,3)	0.00	(1.890,2.110)	1.579

Table 4.2: Validation of BFGS method for optimization

	Actual		BFGS method	
	coordinate	value	coordinate	value
Sphere function	(0,0)	0.00	$(1.30 \times 10^{-12}, -8.06 \times 10^{-7})$	-8.06×10^{-7}
Booth function	(1,3)	1.579	(0.997,2.997)	1.388×10^{-4}

and PSD minimum value whereas table 4.2, provides a comparison between actual minimum value and minimum value obtained by BFGS algorithm. From the tables it is evident that both of these optimization methods are giving reasonable optimized results. The result from PSD can be improved by decreasing the size of steps.

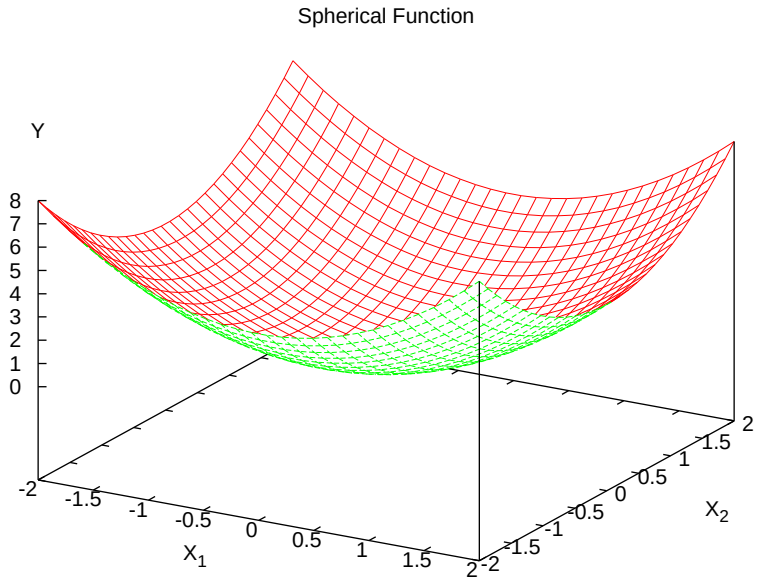

Figure 4.1: Sketch of Sphere function

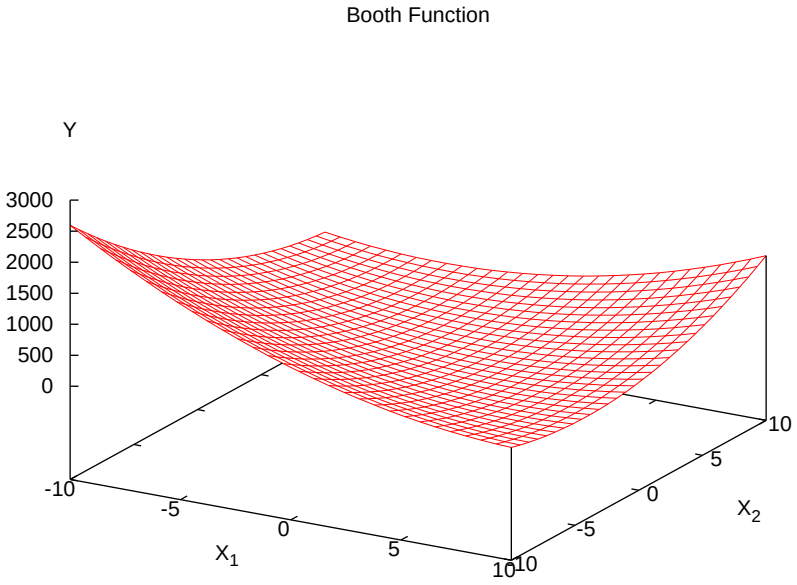

Figure 4.2: Sketch of Booth′s function

4.2 Validation of Kriging

Once the fortran code for optimization is validated, another fortran code is developed for the Kriging method. To validate the Kriging method, both Sphere and Booth's function are employed. In figure 4.3 and figure 4.4, comparison of predicted values and actual values are provided. From these figures it is also understandable that with the increase of number of sample points, the prediction due to Kriging improves. In this work if the number of sample points are more than 40, this Kriging can predict values within very reasonable tolerance. To get an acceptable approximation 40 sample points are used for Kriging.

4.3 Convergence Test for Number of Panels

In this thesis, a panel method based program MAPS resistance is used for calculating the wave making resistance. For this reason before optimization, it is required to go through a convergence test for number of panels on hull. Beside this it is also required to find appropriate dimension of free surface. In this thesis three different types of hulls are used for optimization. The hulls are Wigley(I), Series 60 and KCS container. Convergence tests for number of panels on hull have been carried out for Wigley(I) hull, Series 60 hull and KCS container hull at Froude number 0.300, 0.300 and 0.260 respectively. From figure 4.5 and figure 4.6, it can be seen that the wave making resistance of Wigley(I) and Series 60 converge if the numbers of panels are around 3200 on hulls. The free surface for a ship can be defined by three parameters: forward length (l_f), aft length (l_a) and side length (l_s). To understand the parameters, figure 4.7 has been introduced. Based on the free surface convergence test, the value of the free surface parameters for Wigley(I) hull and Series 60 hull are kept as l_f=1.0 L, l_a=2.25 L and l_s= 1.0 L where L= length of ship hull at waterline.

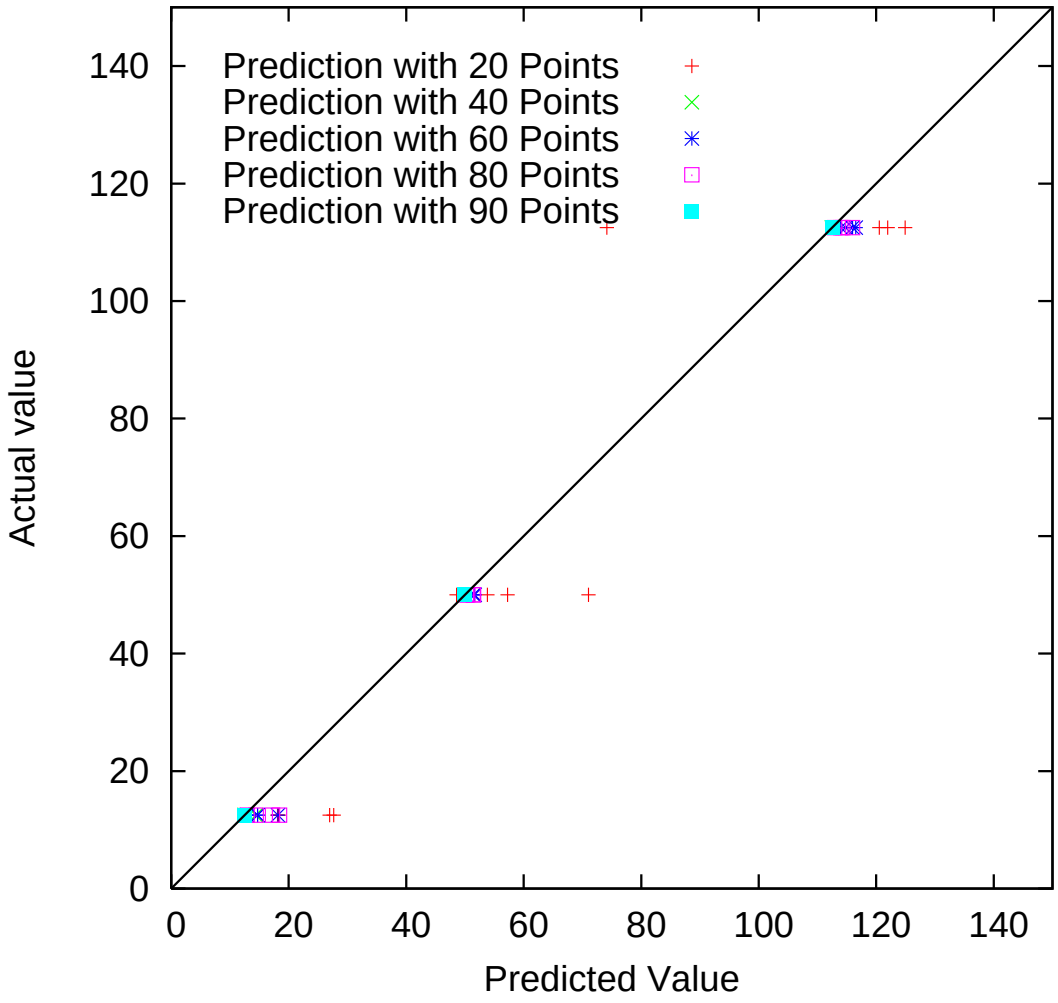

Figure 4.3: Comparison of actual and predicted values for Sphere function

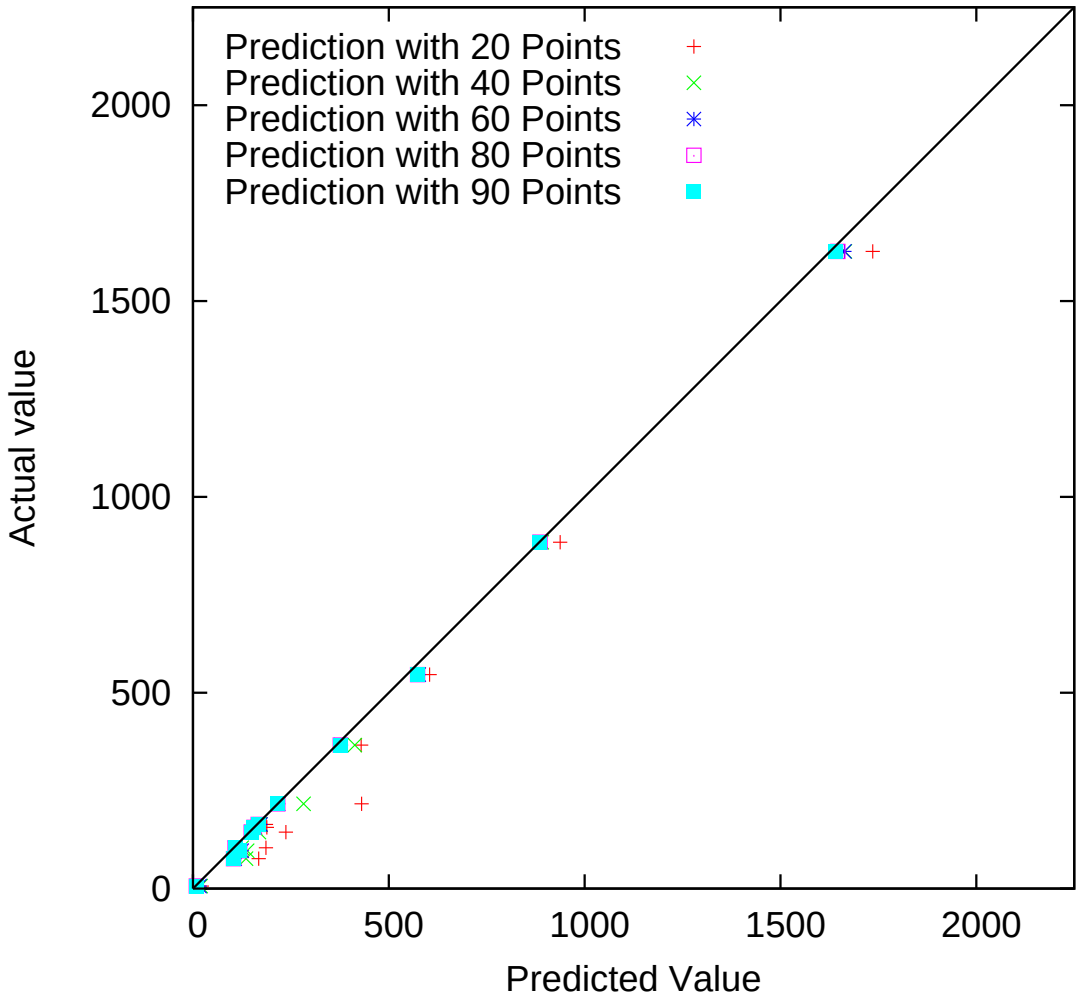

Figure 4.4: Comparison of actual and predicted values for Booth's function

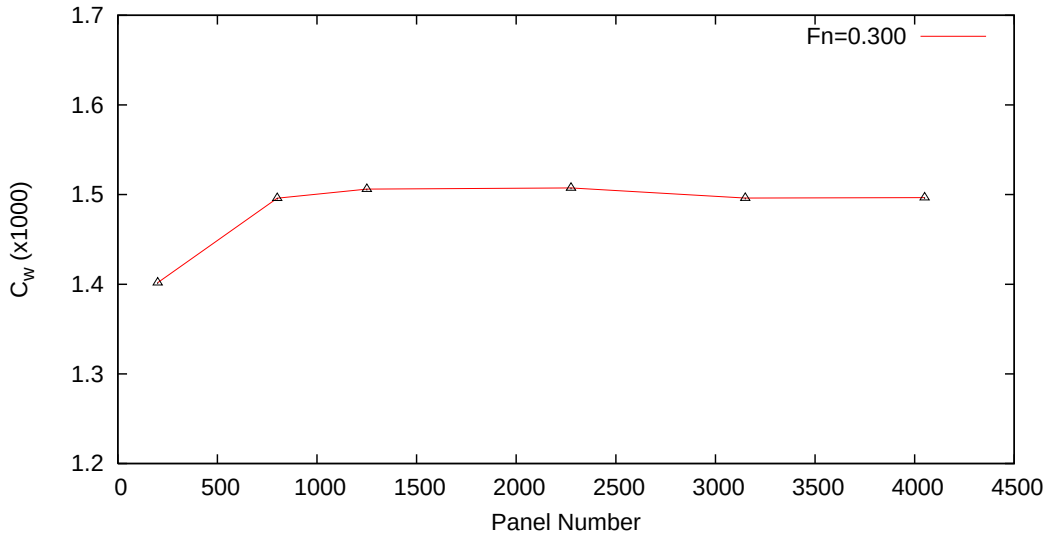

Figure 4.5: Convergence study of panels for Wigley(I) hull

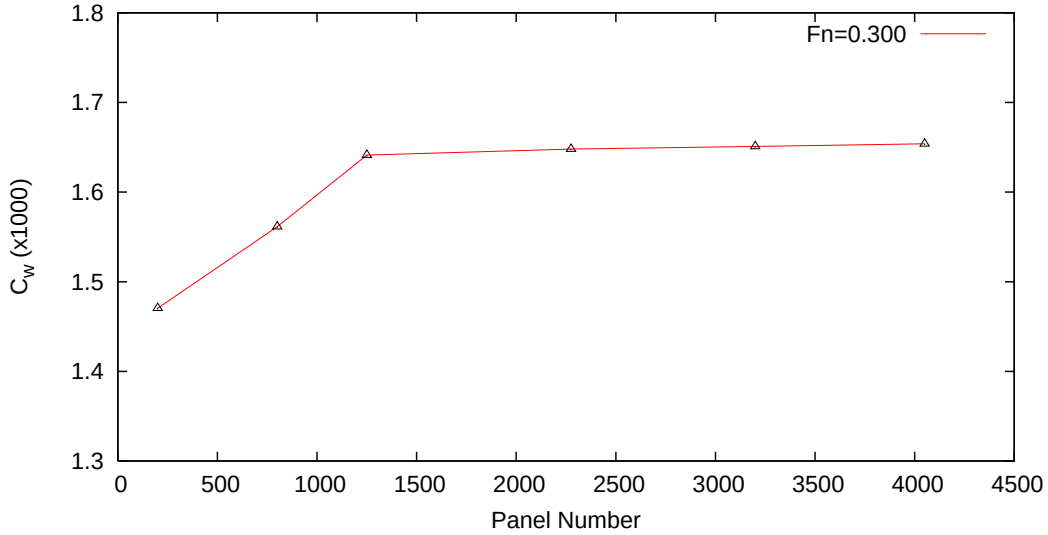

Figure 4.6: Convergence study of panels for Series 60 hull

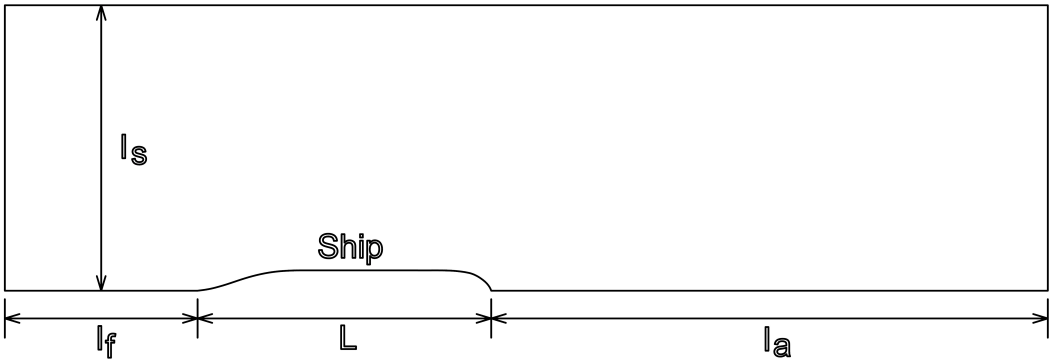

Figure 4.7: Geometry of free surface

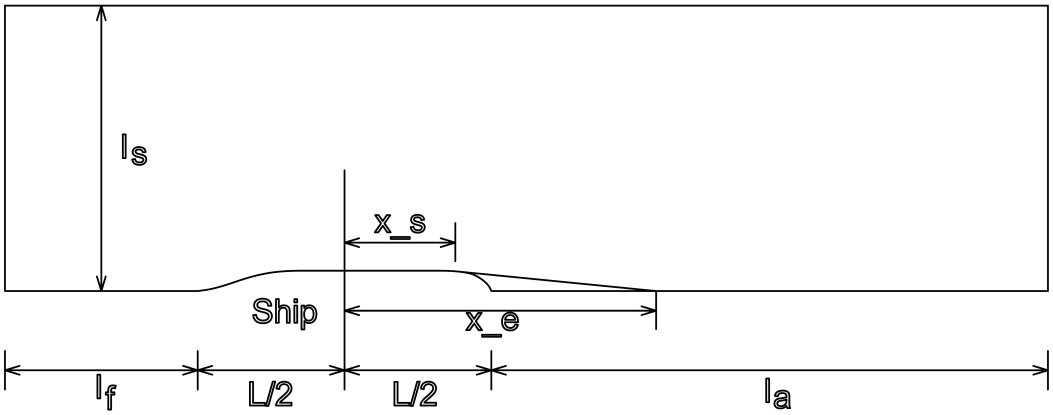

Figure 4.8: Geometry of free surface for KCS container

For KCS container hull a convergence study of number of panels on hull has been carried out. From the study it can be seen that 3600 panels on hull surface is sufficient to predict the wave making resistance (figure 4.9). For the calculation of wave making resistance of KCS container hull, it can be observed that wave contours at the stern region is full of vortices (Peng et al. (2014)). To avoid the computational complexity of this kind of incident, this portion was excluded from the calculation. Though the stern portion was excluded, it still generates reasonable wave making resistance with respect to the experimental value. To understand the exclusion, figure 4.8 is provided where x_s and x_e indicate the starting point and ending point of exclusion respectively. Again a convergence test is also carried out for the free surface of KCS container ship. From the study of free surface convergence, parameters for the KCS container ship are kept as l_f=1.50 L, l_a=2.50 L, l_s= 1.0 L, x_s = 0.42 L and x_e = 2.0 L.

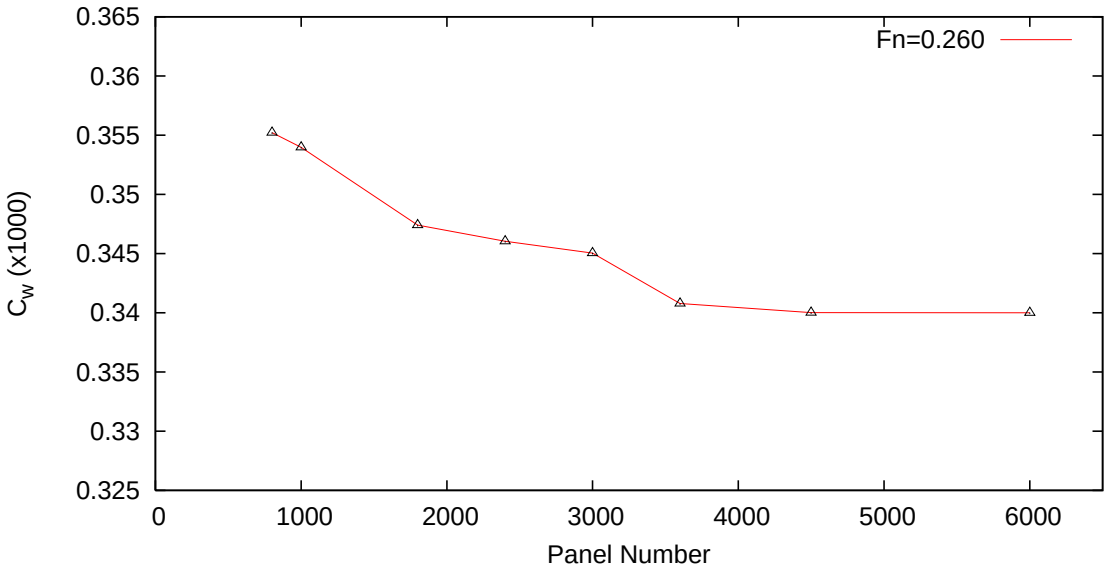

Figure 4.9: Convergence study of panels for KCS container hull

4.4 Comparison of Input Hull Properties

In this thesis the input for optimization technique is an IGES file. The MAPS resistance cannot calculate the wave resistance directly from the IGES file. So it is required to prepare input file from IGES file for MAPS resistance. At the time of input file preparation, ship hull goes through multiple interpolations. So there is a chance that the hull properties get changed. To avoid these kind of problems, cubic spline (Press et al. (1996)) is implemented for interpolation. The dimension of different hulls those are used in this thesis are provided on table 4.3. A comparison of hull properties is provided for different kinds of ship on table 4.4, where it is shown that the area and the volume are almost same before and after the generation of input hull for MAPS.

Table 4.3: Principal particulars of different hulls

	Length at waterline(m)	Breadth(m)	Draft(m)
Wigley(I) Hull	100.00	10.00	6.25
Series 60 Hull	200.00	26.24	10.50
KCS container Hull	307.84	42.62	14.30

Table 4.4: Comparison of ship hull properties before and after the input hull generation

	Properties based on IGES file		Properties based on MAPS input file	
	area(m^2)	volume(m^3)	area(m^2)	volume(m^3)
Wigley(I) Hull	1487.24	2074.15	1486.89	2074.93
Series 60 Hull	6608.15	25953.72	6606	25956.38
KCS container Hull	16723.35	120837.385	16634.66	120516.495

4.5 Comparison of Properties for Optimized Hulls

In this work multiple types of optimization techniques are implemented. Table 4.5 is provided to give a detail explanation of different types of optimized techniques.

Table 4.5: Nomenclature of different types of hull optimization technique

Name	Modification	Optimization	Surrogate model
Original Hull	-	-	-
Optimized Hull(schm:I1)	schm:1	PSD	-
Optimized Hull(schm:K1)	schm:1	BFGS	Kriging
Optimized Hull(schm:K2)	schm:2	BFGS	Kriging
Optimized Hull(schm:K3)	schm:3	BFGS	Kriging

4.5.1 Wigley(I) hull

A Wigley(I) hull is a mathematical hull. If the water line, breadth and draft of the ship are represented by L, B and T; the coordinates of Wigley(I) hull can be represented by equation 4.3 (Tarafder and Suzuki (2008)).

$$y(x,z) = \frac{B}{2}(1-(\frac{z}{T})^2)(1-\frac{4x^2}{L^2}) \tag{4.3}$$

4.5.1.1 Wigley(I) Hull Optimization with schm:1

In this optimization method, the hull surface is changed depending on two variables. The variables are w_f and w_a (equation 3.12); the range of variables are provided on equation 4.4. It can be mentioned here that the maximum and the minimum values of these two variables will be less than '1' and more than '-1' respectively. Because of this method, all the surface points go through modification resulting the global hull modification.

$$-0.4 \leq w_f \leq 0.4, -0.4 \leq w_a \leq 0.4 \tag{4.4}$$

In this method, the path of steepest descent (PSD) is used to optimize the hull. As it is a method of searching the path of steepest descent, it takes numerous iteration to obtain the final result. Later on Kriging method is introduced to reduce the running time of the program. With Kriging a new and updated optimization method named as BFGS method is used. For the method of steepest descent and Kriging, it is supposed to get same result as the hull deformation procedure is same. But normally it does not happen as Kriging is a statistical method for predicting the value of unknown point based on the surrounding known points values. Beside this the selection of sampling model also plays important role on predicting values by Kriging. Based on Kriging, the whole scenario within the limit of variables can be predicted. By changing the value of variables from maximum to minimum a surface plot is generated on figure 4.10 where if v_1=0.0 then $w_f = -0.4$ and if v_1=1.0 then $w_f = 0.4$. Similarly if v_2=0.0 then $w_a = -0.4$ and if v_2=1.0 then $w_a = 0.4$. At the time of applying schm:1 method, principal particulars of the ship hull are kept fixed.

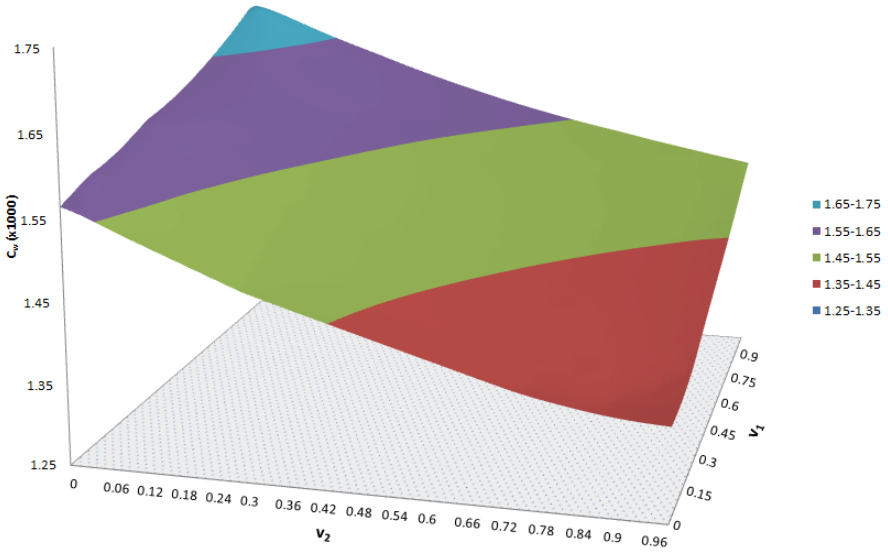

Figure 4.10: Wave making resistance (C_w) based on Kriging for Wigley(I) hull (schm:K1)

4.5.1.2 Wigley(I) Hull Optimization with schm:2

In this optimization technique, a certain region of the hull is modified within a range to obtain a optimized hull. The surface points associated with the region go through a movement to achieve the required hull modification. Unlike schm:1, in this case the principal particulars also remain unchanged. As per equation 3.17, there are four variables x_1, x_2, a_1 and a_2 associated with this method. For this case the values of x_1 and x_2 are kept as $0.5L$ and $1.0L$ respectively where L indicates the length of ship at waterline. The range of a_1 and a_2 are kept within the following limit, $-0.020L \leq a_1 \leq 0.0$ and $0.675L \leq a_2 \leq 0.775L$.

4.5.1.3 Wigley(I) Hull Optimization with schm:3

The target of this optimization technique is to reduce wave making resistance by introducing a bulbous bow. There are six variables associated with this hull modification method. There is no fixed limit of these variables. But based on table 3.1 and table 3.2, a set of limits are set for the Wigley(I) hull on table 4.6. Unlike schm:1 and schm:2, the principal particulars are kept unchanged. An optimized hull is obtained from this optimization technique. In schm:K3 bulbous bow is generated on the front side of the hull. For better understanding of this hull modification method figure 4.11 is provided where the comparison of profile sections and waterlines are illustrated.

Table 4.6: Range of parameters for bulb geometry for Wigley(I) hull

Parameters	Symbol	Ratio	Minimun	Maximum
Linear coeff	C_{LPR}	L_{PR}/L	0.0180	0.0310
Breadth coeff	C_{BB}	B_b/B	0.1630	0.2249
Depth coeff	C_{ZB}	Z_B/T	0.2624	0.5584
Lateral coeff	C_{ABL}	A_{BL}/A_{Mid}	0.1625	0.3263
Trans.Area coeff	C_{ABT}	A_{BT}/A_{Mid}	0.1310	0.2049
Volume coeff	C_{VPR}	V_{PR}/V	0.002287	0.006747

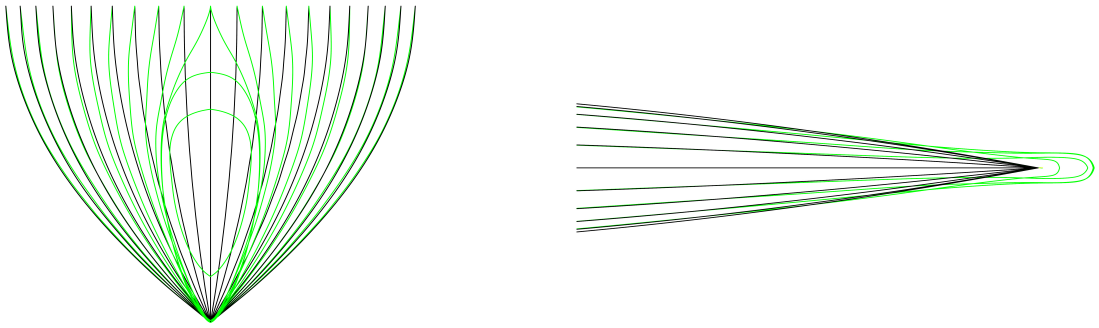

(a) Comparison of forward sections of original Wigley(I) hull (Black) and optimized Wigley(I) hull (Green)

(b) Comparison of waterlines at bow region of original Wigley(I) hull (Black) and optimized Wigley(I) hull (Green)

Figure 4.11: Comparison of Wigley(I) hull and optimized Wigley(I) hull

4.5.1.4 Comparison of Properties of Optimized Wigley(I) Hulls

Based on two optimization algorithm and three hull modification methods, four optimized hulls are generated. In PSD, the wave making resistance of optimized hull is achieved directly from the MAPS resistance. But for BFGS method the wave making resistance of optimized hull is achieved based on the Kriging. So there is a chance to get little deviated result in Kriging method from directly calculated wave making resistance. A comparison of predicted and actual wave making resistance is provided on table 4.7. The table shows that predicted and calculated results are in good agreement. Table 4.8 gives a comparison of volume, area and location of center of buoyancy (LCB) for original and optimized Wigley(I) hulls. From the tables it can be mentioned here that the change in volume, area and location of center of buoyancy of the ships are within a tolerable limit whereas all hull modification methods are generating hull with lesser wave making resistance than the original hull. Compared to other hull modification methods at Froude number 0.300, schm:K3 is giving the best result for Wigley(I) hull. In terms of wave making resistance this method is producing 31.90% improved result whereas the change on volume, area and LCB are

2.70%, 2.37% and 1.27% respectively. Although schm:K1 and schm:K2 are not generating better result than schm:K3, but still these two methods are generating improved results than original Wigley(I) hull. For schm:K1, 9.28% improvement is achieved on wave making resistance by changing 3.50% of volume, 0.71% of area and 0.103% of LCB. For schm:K2, the improvement in wave making resistance is 5.20% whereas the change in volume, area and LCB are 2.10%, 0.46% and 0.67% respectively.

Table 4.7: Comparison of predicted and actual C_w for different optimized Wigley(I) hulls at Froude number 0.30

	Predicted C_w(x1000)	Calculated C_w(x1000)
Experimental value	-	1.555
Original Hull	-	1.498
Optimized Hull(schm:I1)	-	1.417
Optimized Hull(schm:K1)	1.369	1.359
Optimized Hull(schm:K2)	1.426	1.420
Optimized Hull(schm:K3)	1.028	1.020

Table 4.8: Comparison of Wigley(I) hull properties before and after optimization

	Volume(m^3)	Area(m^2)	LCB(m),+ on aft
Original Hull	2074.15	1487.24	0.00
Optimized Hull(schm:I1)	2051.53	1483.34	-0.9658
Optimized Hull(schm:K1)	2001.50	1476.59	0.1033
Optimized Hull(schm:K2)	2030.61	1480.34	0.6729
Optimized Hull(schm:K3)	2130.24	1522.60	-1.267

4.5.1.5 Comparison of Wave Making Resistance of Optimized Wigley(I) Hulls

The optimization is carried out for the Froude number 0.300. A comparison of hull sections of optimized Wigley(I) hulls are illustrated on figure 4.12. For all optimized hulls sections are smooth enough to be realistic ship hulls. Based on the optimized hulls a series of wave making resistances are calculated at different Froude numbers.

In figure 4.13, the comparison of optimized hulls with the experimental and original hull results is provided. Within the range of Froude number 0.230 to 0.370, all optimized hulls are producing lesser wave making resistance than experimental and original Wigley(I) hull. For the range of Fn= 0.370 to Fn= 0.425, optimized hull (schm:K1) create higher wave making resistance than original hull but in this range other optimized hulls generate reduced wave making resistance. At higher Froude number($\geqslant$ 0.425) all the hulls create either equal or higher wave making resistance. A comparison hull sections of original and optimized Wigley(I) hulls is provided on figure 4.12. From the comparison of wave profiles on hull in figure 4.14 and 4.15, it is also visible that the hull which generates lesser wave making resistance has shorter wave hight at bow.

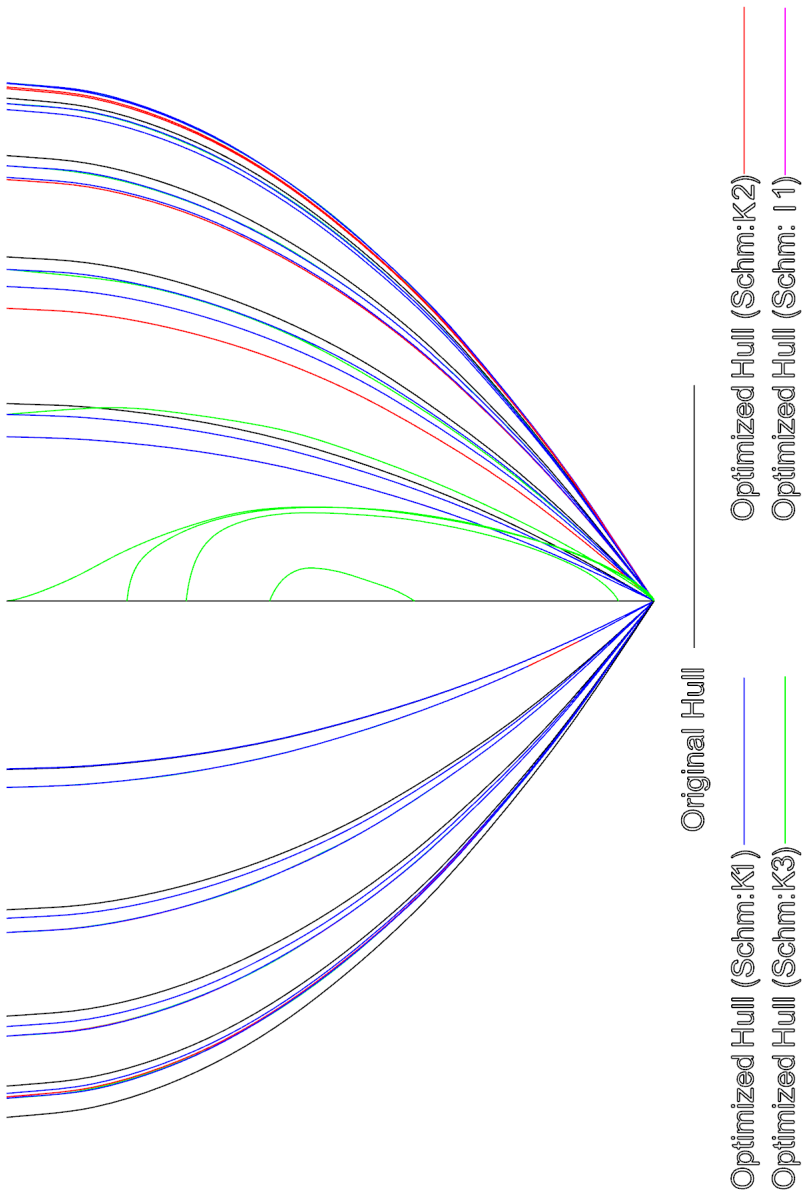

Figure 4.12: Comparison of sections for different Wigley(I) hulls

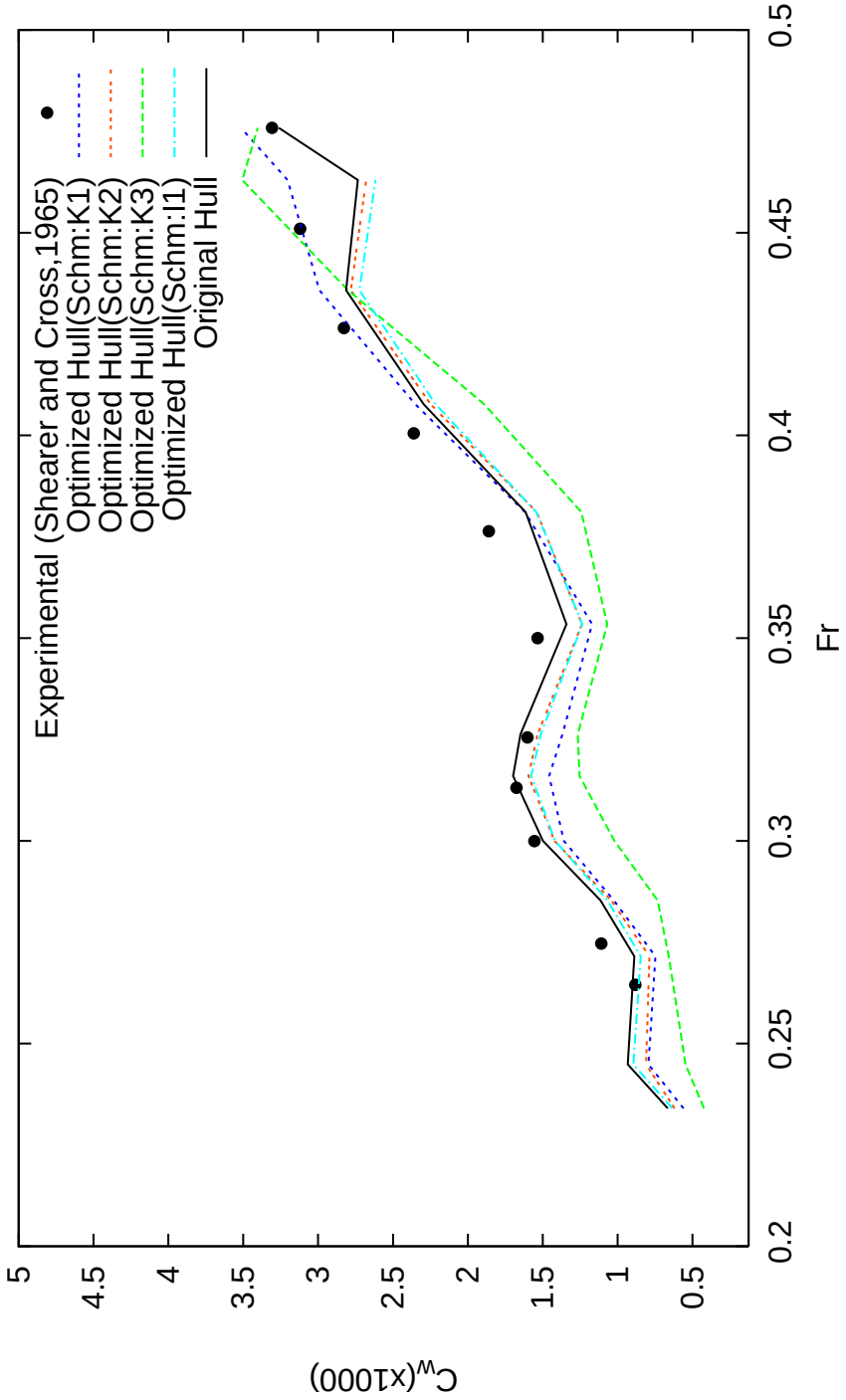

Figure 4.13: Comparison of C_w of experimental, calculated and optimized Wigley(I) hulls

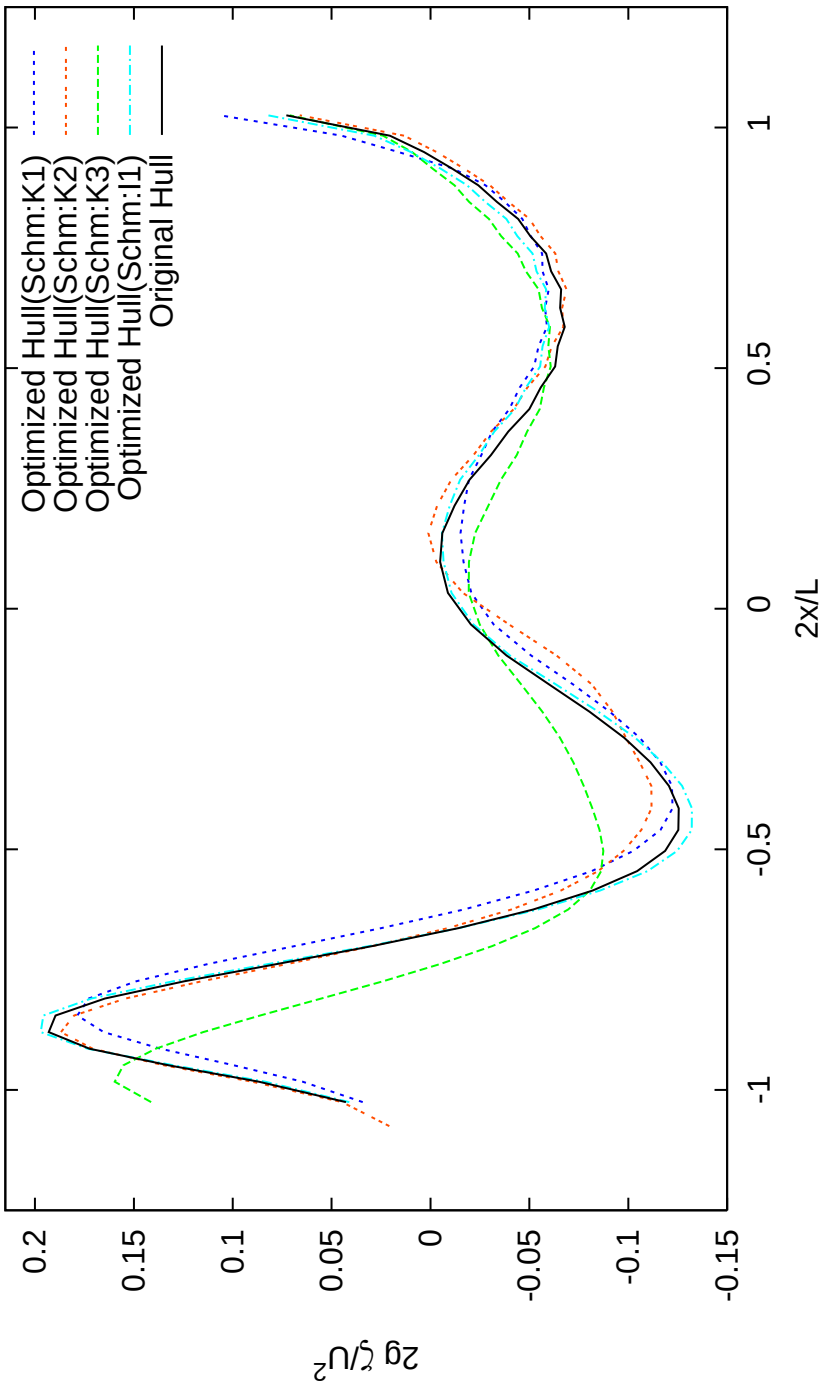

Figure 4.14: Comparison of wave profile on hull surface for different types of Wigley(I) hulls (Fr=0.300)

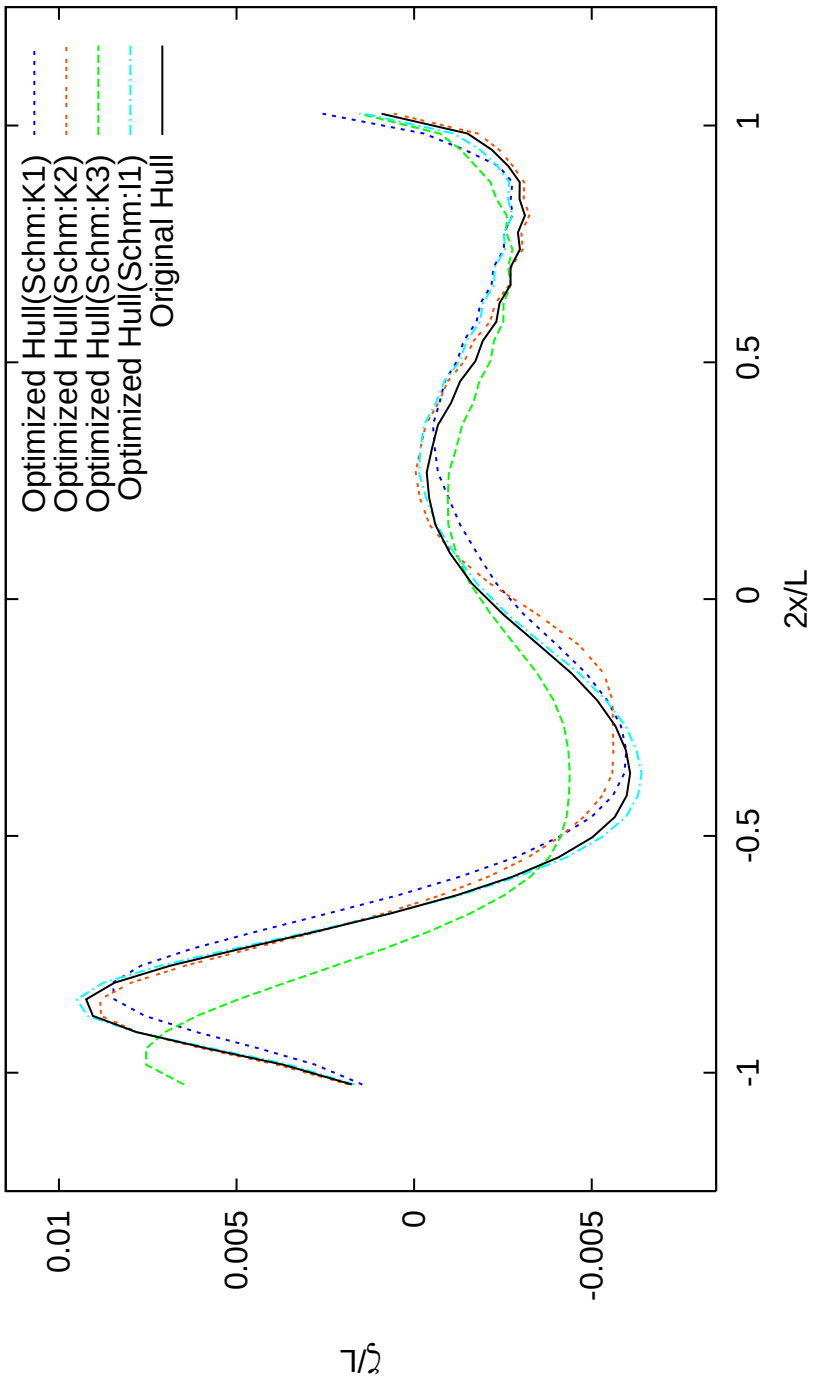

Figure 4.15: Comparison of wave profile on hull surface for different types of Wigley(I) hulls (Fr=0.316)

4.5.2 Series 60 hull

Series 60 is one of the most used hull form for researchers to investigate the optimization of ship hull. The optimization for series 60 hull is carried out at its design speed ($F_n = 0.316$). The length of ship at load waterline, breadth and draft for series 60 are taken as 200 m, 26.24 m and 10.5 m respectively.

4.5.2.1 Series 60 Hull Optimization with schm:1

Unlike Wigley(I), in this optimization procedure the number of variables are kept two. The variables are w_f and w_a (equation 3.12); the range of the variables are provided on equation 4.5. It can be mentioned here that the maximum and minimum values of these two variables will be less than '1' and more than '-1' respectively.

$$-0.3 \leq w_f \leq 0.3, -0.3 \leq w_a \leq 0.3 \tag{4.5}$$

Two different kinds of optimization procedures are introduced here. At first PSD is used to optimize the hull. Later on BFGS method is implemented to optimize the hull by using Kriging method.

4.5.2.2 Series 60 Hull with schm:2

In this procedure Kriging with BFGS algorithm is selected to modify a certain region of the hull within a range to obtain optimized hull. As per equation 3.17, there are four variables x_1, x_2, a_1 and a_2 associated with this method. For this case the values of x_1 and x_2 are kept as $0.5L$ and $1.0L$ respectively. The range of a_1 and a_2 are kept within the following limit, $-0.03L \leq a_1 \leq 0.03L$ and $0.750L \leq a_2 \leq 0.840L$. At the time of hull modification, principal particulars of the hull are kept fixed.

4.5.2.3 Series 60 Hull with schm:3

Unlike Wigley(I) hull, schm:3 is used for generating bulbous bow for reducing the wave making resistance. In this hull modification procedure six variables are changes within a range based on table 3.1 and table 3.2 to optimize the hull. The ranges of hull variables are provided in table 4.9. In schm:K3 bulbous bow is generated on the bow region of the hull. For better understanding of this modification, figure 4.16 is provided where the section and waterlines are illustrated.

Table 4.9: Range of parameters of bulb geometry for Series 60 hull

Parameters	Symbol	Ratio	Minimun	Maximum
Linear coeff	C_{LPR}	L_{PR}/L	0.0050	0.0300
Breadth coeff	C_{BB}	B_b/B	0.0500	0.1300
Depth coeff	C_{ZB}	Z_B/T	0.2600	0.5700
Lateral coeff	C_{ABL}	A_{BL}/A_{Mid}	0.0198	0.1587
Trans.Area coeff	C_{ABT}	A_{BT}/A_{Mid}	0.0353	0.0870
Volume coeff	C_{VPR}	V_{PR}/V	0.00023	0.002304

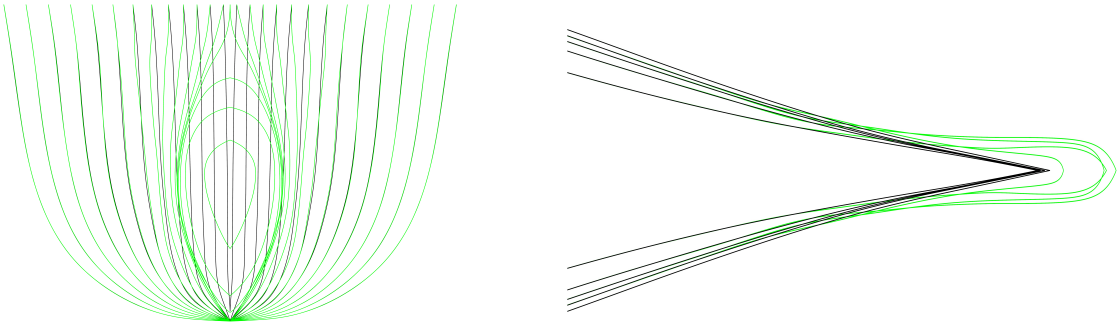

(a) Comparison of forward sections of original Series 60 hull (Black) and optimized Series 60 hull (Green)

(b) Comparison of waterlines at bow region of original Series 60 hull (Black) and optimized (schm:3) Series 60 hull (Green)

Figure 4.16: Comparison of original Series 60 hull and optimized Series 60 hull

4.5.2.4 Comparison of Properties of Optimized Series 60 Hulls

For series 60 hull, the optimization is conducted at the Froude number 0.316. Based on four different combinations optimized hulls are generated. Unlike Wigley(I), there is small deviation for optimized results obtained from PSD with schm:1 and Kriging method based BFGS with schm:1. A comparison of predicted wave making resistance and directly calculated wave making resistance is given on table 4.10. The table shows that predicted and calculated results are in good agreement. Table 4.8 gives a comparison of volume, area and location of center of buoyancy (LCB) for original and optimized Series 60 hulls. From the tables, it can be mentioned here that the change in volume, area and location of center of buoyancy of ships are within a tolerable limit whereas all hull modification methods are generating hulls with lesser wave making resistance than the original hull. Compared to other hull modification methods, schm:K2 is giving the best result. In terms of wave making resistance this method reduced the resistance by 22.51% whereas the change on volume, area and LCB are 2.30%, 1.30% and 0.47% respectively. Compared to original hull, schm:k3 is also generating improved result by reducing 20.34% of wave resistance. The reduction due to schm:K1 and schm:I1 are not as good as like the other two hull modification methods but still these they are generating 8.65% and 9.89% reduction in wave making resistance respectively.

Table 4.10: Comparison of predicted and actual C_w for different optimized Series 60 hulls

	Predicted C_w(x1000)	Calculated C_w(x1000)
Original Hull	-	1.6132
Optimized Hull(schm:I1)	-	1.4536
Optimized Hull(schm:K1)	1.4927	1.4742
Optimized Hull(schm:K2)	1.2009	1.2500
Optimized Hull(schm:K3)	1.2681	1.2850

Table 4.11: Comparison of Series 60 hull properties before and after optimization

	Volume(m^3)	Area(m^2)	LCB(m),+ on aft
Original Hull	25953.72	6608.15	0.189
Optimized Hull(schm:I1)	25675.29	6576.01	0.195
Optimized Hull(schm:K1)	25544.41	6562.51	0.195
Optimized Hull(schm:K2)	25356.77	6522.05	0.6653
Optimized Hull(schm:K3)	26199.647	6707.38	-0.667

4.5.2.5 Comparison of Wave Making Resistance of Optimized Series 60 Hulls

A comparison of hull sections of optimized Series 60 hulls are illustrated on figure 4.17. Based on the optimized hulls a series of wave making resistances are calculated at different Froude numbers (Fn). Beside this, experimental results from Ishikawajima-Harima heavy Industries Co., Ltd.(IHHI) and University of Tokyo are also provided to compare the optimized resistance (Tarafder and Suzuki (2008)). In figure 4.18, the comparison of wave making resistance of optimized hulls with the experimental and original Series 60 hull is provided. From the figure it is visible that the reduction of wave making resistance for optimized hulls are not significant for Froude number 0.100 to 0.260. From the range of 0.260 to 0.340 all optimized hulls are producing improved results. After this range optimized hull (schm:K2) and optimized hull (schm:K3) are showing improved performances in term of wave making resistance. From wave profiles of these hulls in figure 4.19, it is also understandable that the hull which generates lesser wave making resistance has shorter wave hight at bow. A comparison of wave profiles on hulls are provided on figure 4.19 for the Froude number 0.316.

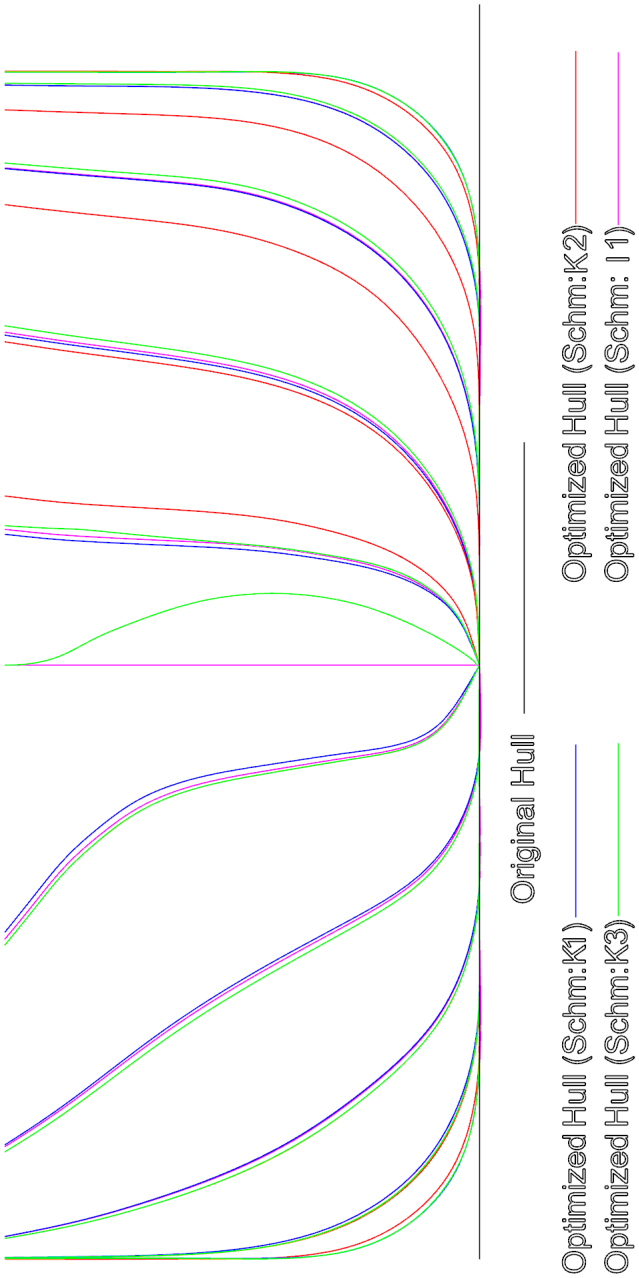

Figure 4.17: Comparison of sections for different Series 60 hulls

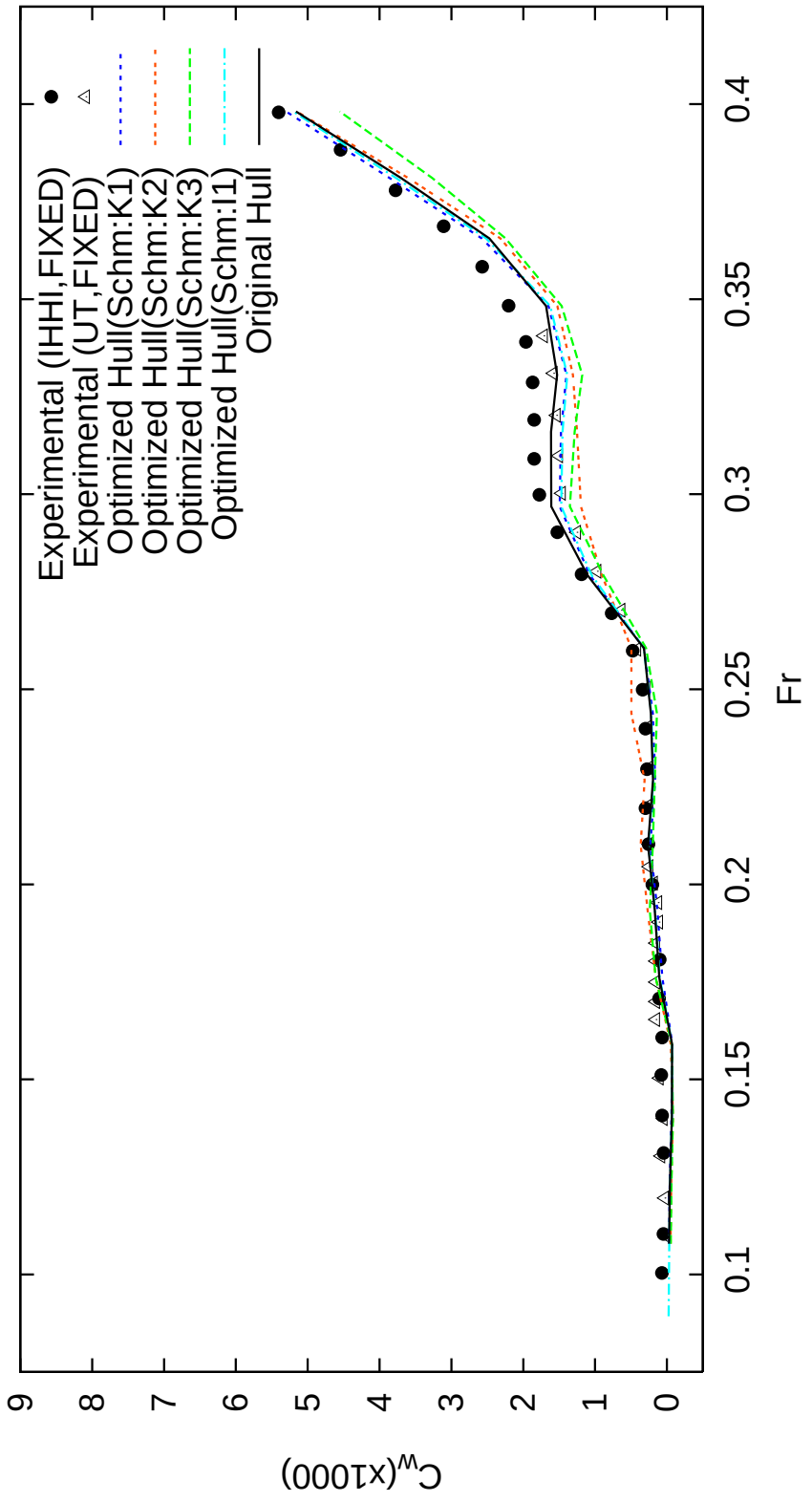

Figure 4.18: Comparison of C_w of experimental, calculated and optimized Series 60 hull

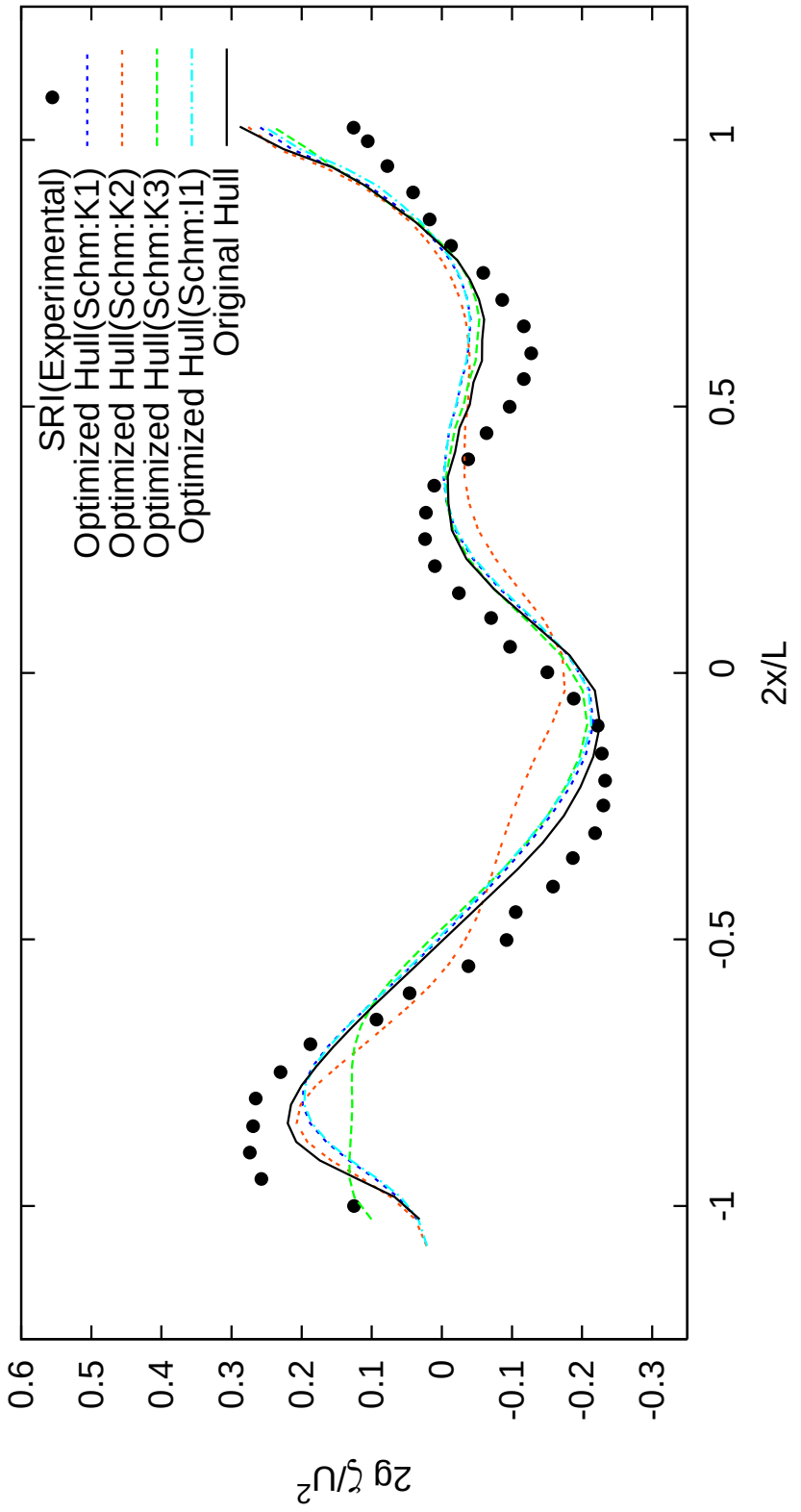

Figure 4.19: Comparison of wave profile on hull for experimental, calculated and optimized Series 60 hull (Fr = 0.316)

4.5.3 KCS Container Hull

KCS container has large bulbous bow and blunt stern. Unlike Wigley(I) and Series 60 hull both schm:1 and schm:2 are applicable for this hull. Schm:1 is a kind of shifting methods. As the parallel middle body of this hull is comparatively longer than Series 60 hull, the schm:1 will have less effect on reducing the wave making resistance on this hull. For this reason only schm:2 is applied to KCS container hull to optimize the wave making resistance.

4.5.3.1 KCS Container Hull Optimization with schm:2

Unlike Wigley(I) hull and Series 60 hull , in this modification method the forward part of the hull is modified. The number of variables are kept two. The variables are a_1 and a_2 (equation 3.17); the range of the variables are provided on equation 4.6 where the L indicating the length of ship at waterline.

$$-0.03L \leq a_1 \leq 0.02L, 0.75L \leq a_2 \leq 0.885L \tag{4.6}$$

To optimize the hull, BFGS method is implemented with the help of Kriging method.

4.5.3.2 Comparison of Properties of Optimized KCS Container Hull

For KCS container hull, based on schm:2 the optimization is conducted at Froude number 0.260 and 0.300. For the sake of simplicity, KCS container hull optimized at Froude number 0.26 and KCS container hull optimized at Froude number 0.30 can be expressed as 'OKCS26' and 'OKCS30' respectively. The prediction of resistance by Kriging for this ship hull is carried out based on 40 sample points. Comparisons of predicted wave making resistance and calculated wave making resistance are given on table 4.12 and table 4.13. The tables show that predicted and calculated results

for OKCS26 and OKCS30 are in good agreement. The comparison of volume, area and location of center of buoyancy (LCB) for original and optimized KCS container hulls are provided on table 4.14 where it can be shown that the change in volume, area and location of center of buoyancy of the ships are within a tolerable limit whereas schm:2 is generating hull with lesser wave making resistance than the original hull. A comparison of sections of original hull and optimized KCS container hulls are illustrated on figure 4.20.

Table 4.12: Comparison of predicted and actual C_w for original and OKCS26 hull

	Predicted C_w(x1000)	Calculated C_w(x1000)
Original Hull	-	0.3408
Optimized Hull(schm:K2)	0.2759	0.2857

Table 4.13: Comparison of predicted and actual C_w for original and OKCS30 hull

	Predicted C_w(x1000)	Calculated C_w(x1000)
Original Hull	-	1.397
Optimized Hull(schm:K2)	1.119	1.115

Table 4.14: Comparison of KCS container hull properties before and after optimization

	Volume(m^3)	Area(m^2)	LCB(m),+ on aft
Original Hull	120837.385	16723.350	-0.54
OKCS26	119418.309	16615.605	0.10
OKCS30	119179.108	16597.635	0.26

4.5.3.3 Comparison of Wave Making Resistance of KCS Container Hull

A series of total resistance for original hull is calculated and compared with the experimental and CFD results by Banks et al. (2010) and Larsson et al. (2003). This comparison shows that the calculated total resistance is in good agreement with experimental and CFD results.

Later on based on the optimized hulls, a series of wave making resistances are calculated at different Froude numbers and compared with the original KCS container hull wave making resistance (figure 4.22). From the comparison, it is visible that OKCS26 and OKCS30 generate almost identical wave making resistance at different Froude numbers though their hull sections are not identical (figure 4.20). From Froude number 0.1 to 0.30, the optimized hulls generate reduced wave making resistance than the original hulls. The optimized hulls create higher reduction from Froude number 0.175 to 0.245 and 0.270 to 0.300. From wave profiles of these hulls in figure 4.23 and 4.24, it is also understandable that hulls generating lesser wave making resistance has shorter wave hight at bow. In terms of wave making resistance, for OKCS26 hull at Froude number 0.26, this procedure reduced the resistance by 16.16% whereas the change on volume is 1.174% and for OKCS30 hull at Froude number 0.30, the reduction in wave making resistance is 20.186% whereas the change in volume is 1.37%.

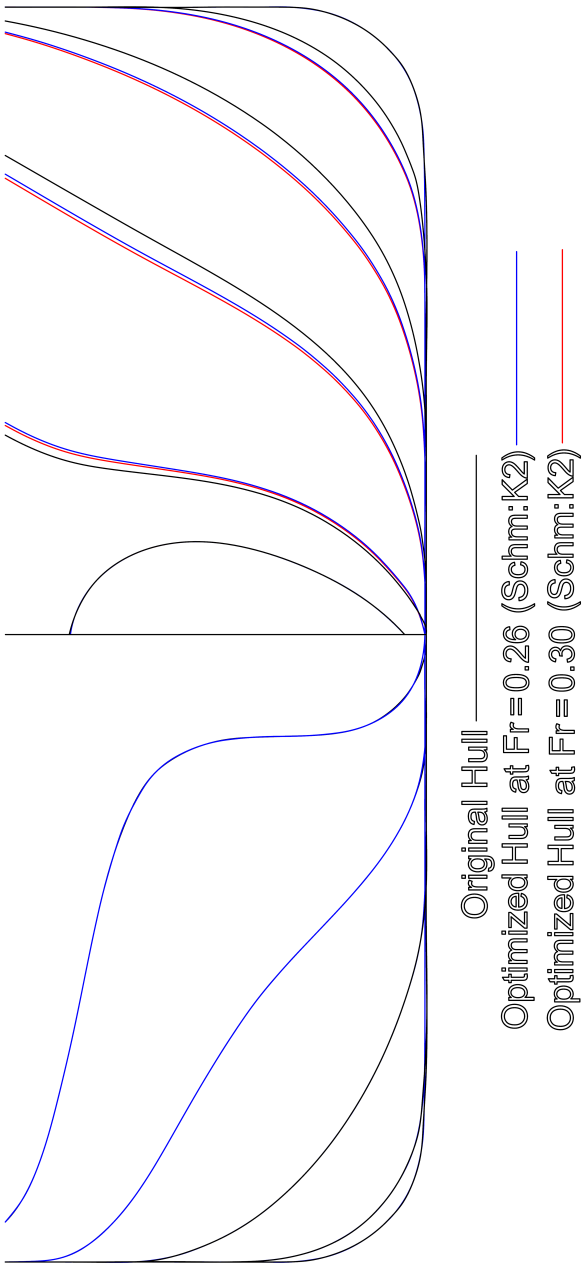

Figure 4.20: Comparison of sections for different KCS container hulls

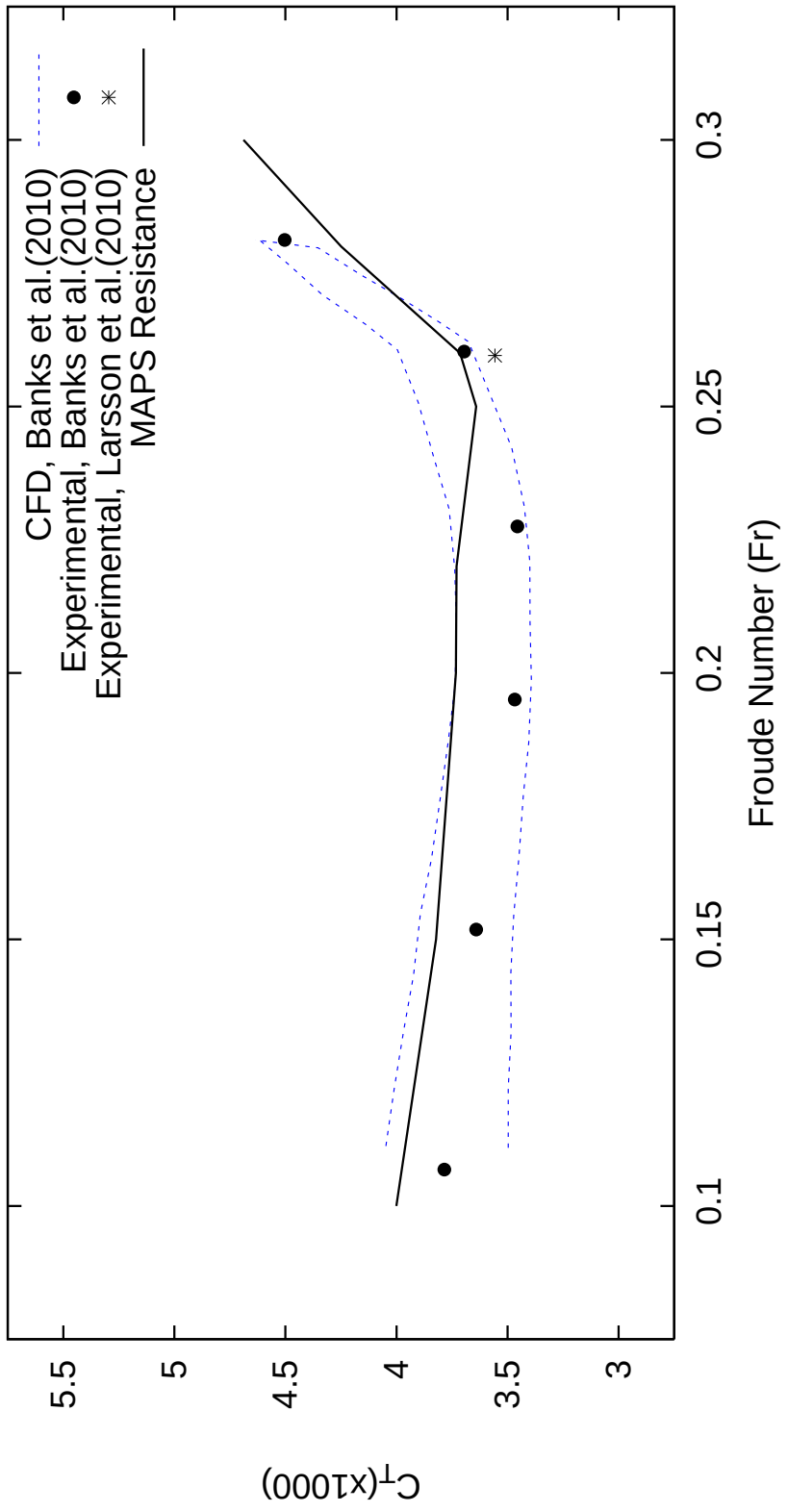

Figure 4.21: Total resistance of KCS container hull

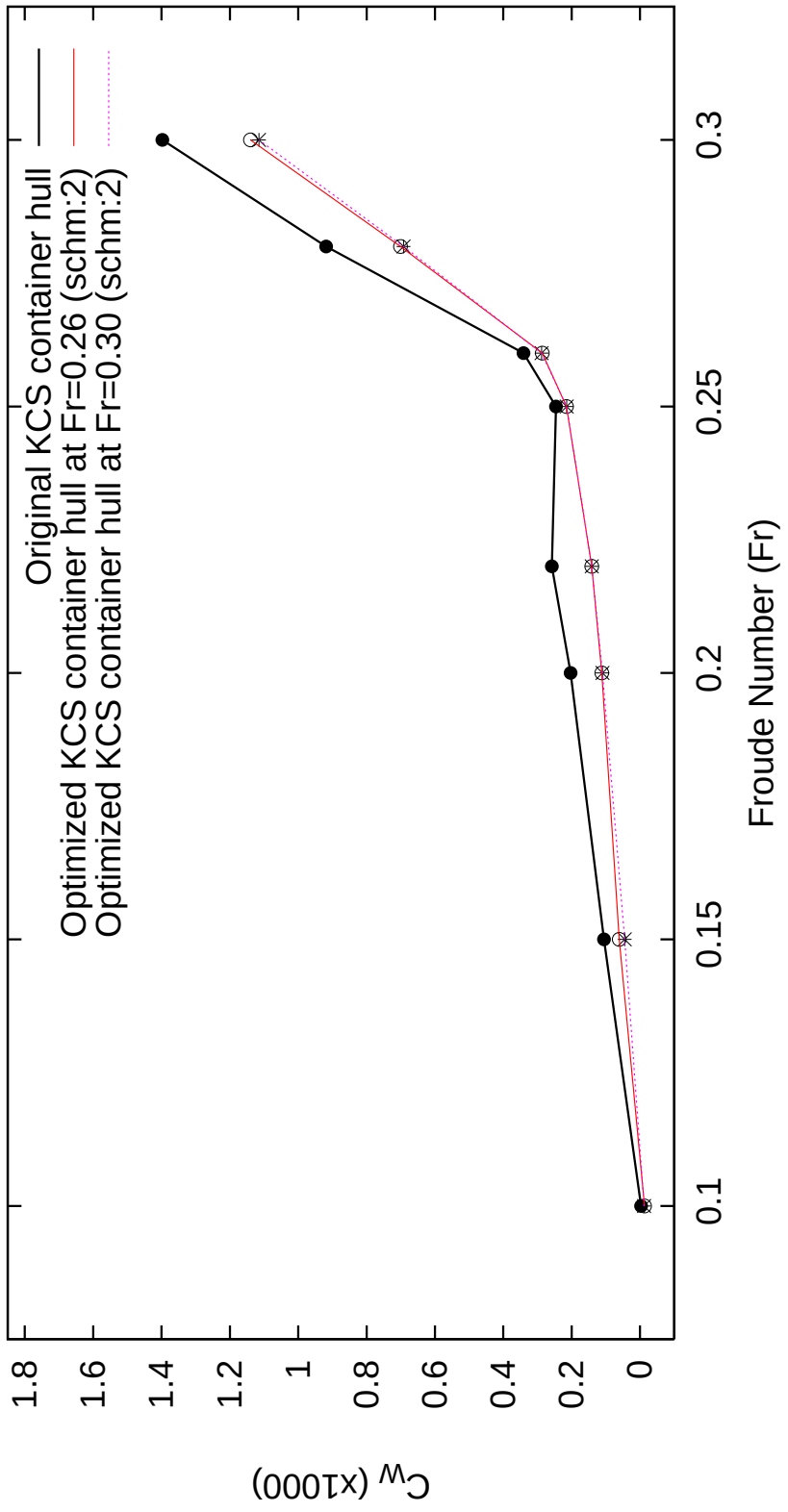

Figure 4.22: Comparison of C_w of original and optimized KCS container hulls

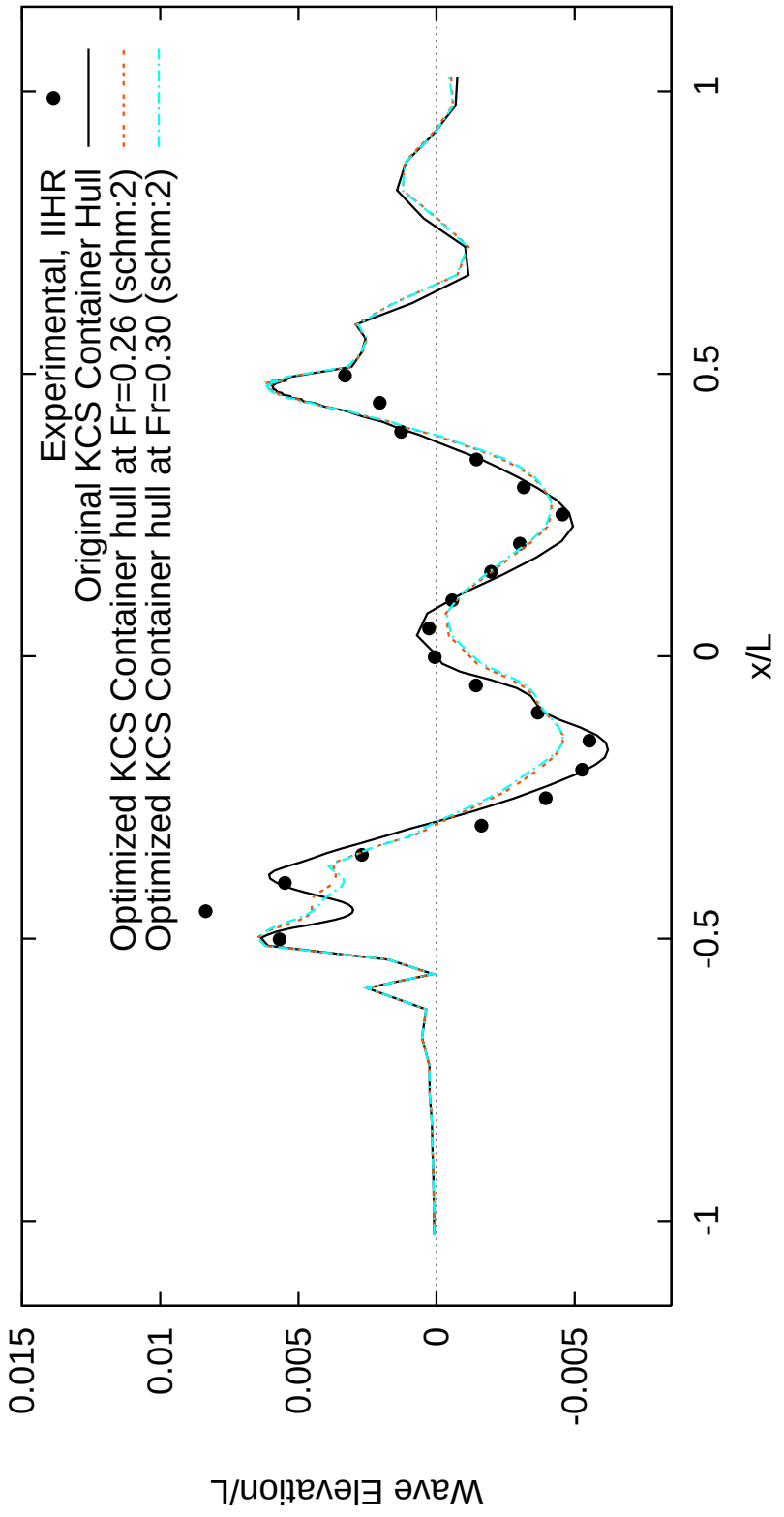

Figure 4.23: Comparison of wave profile on hull for original and optimized KCS Container hull (Fn=0.26)

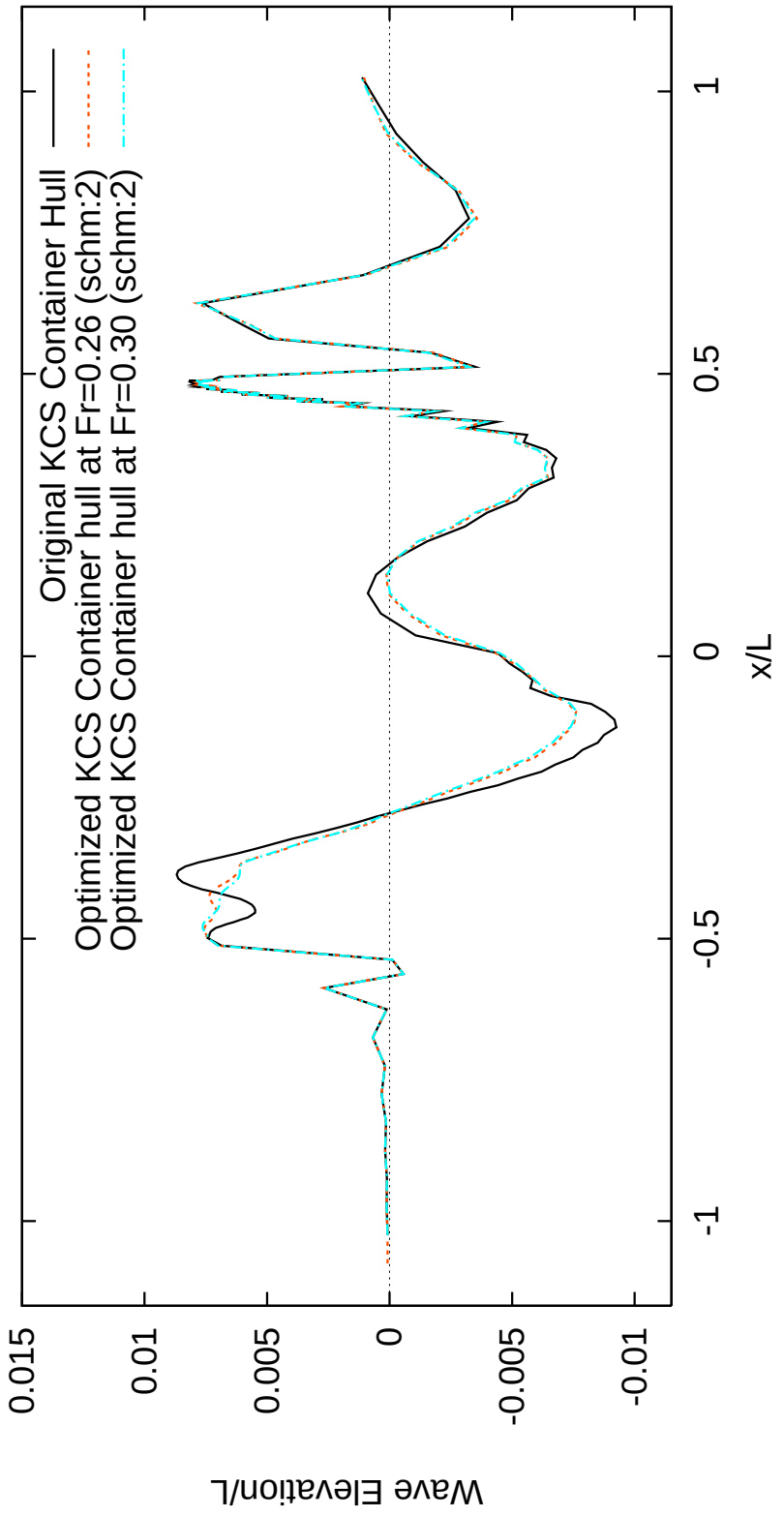

Figure 4.24: Comparison of wave profile on hull for original and optimized KCS Container hull (Fn=0.30)

Chapter 5

Conclusions and Future Work

In this thesis a technique for ship hull optimization based on wave making resistance is developed. The technique starts from reading an IGES file. After interpolation an input point cloud is generated. In this work the hull is optimized based on the wave making resistance. A panel based wave making resistance calculation program MAPS Resistance is used. As per the requirement of the input file of MAPS, the input point cloud is distributed. To optimize a ship hull it is require to modify the ship geometry. Three different types of hull modification methods are applied with two different types of optimization algorithms. At first path of steepest descent is used to optimize the ship hull. With the increment of variables, this algorithm consumes a significant amount of time. To avoid this problem the optimization scenario is mimicked by Kriging method. Later on another optimization algorithm known as Broyden Fletcher Goldfarb Shanno (BFGS) is used to optimized the hull based on the response from Kriging. Multiple validation tests are provided for every step of this optimization technique. Optimization is carried out for Wigley(I), Series 60 and KCS container hull. A comparison of wave making resistance for multiple ship is provided. At the time of generating surface points from NURBS, equally spaced and chord

length methods for parameter selection are employed. If the ship geometry is very complex, an upgraded parameter selection method known as centripetal method can be introduced for parameter calculation.

A random number based Latin Hypercube Design (LHD) is used for Kriging. There is different kinds of LHD. To reduce the number of sample points for Kriging, a better LHD algorithm can be introduced.

On schm:3, bulbous bow is generated for reducing the wave making resistance that makes some part of hull unsmooth. A simple smoothing algorithm named Gaussian algorithm is deployed to solve the problem. A better smoothing algorithm like kalman filter, kernel smoother etc. can be introduced to obtain better result.

If there is multiple patches in IGES file, it is required to combines them together into one patch for this optimization technique. But the current technique can only combine vertically aligned patches. To represent complex ship hull like DTMB or Swath, it needs horizontally aligned patches also. In future work, this optimization technique can be modified to handle multiple directional patches at the time of hull optimization.

BFGS and path of steepest descent are used in this work to optimize the ship hull. These optimization algorithms perform well on local perspective. A global optimization method like genetic algorithm can be introduced to detect an optimized hull on global perspective.

In this thesis different optimized hulls are achieved based on a panel based wave making resistance calculation procedure. To validate the resistance a CFD and model test experiment can be carried out for optimized hull.

There are multiple methods to modify ship hull geometry. Recently parametric ship design is getting the attention from the researchers. In future work a parametric hull modification procedure can be integrated with the current optimization technique to

optimize the ship hull.

In this work, the modification in hull geometry is minimal that ensure the adequate space for machineries after hull optimization. In future work the added wave resistance, seakeeping performance, combined engine and propeller performance can be included on this optimization technique.

Finally, the present optimization technique can also be used for other objective functions related to ship design. To optimize multiple objectives, a multi-objective multivariable optimization strategy can be introduced to replace the present optimization technique.

Bibliography

Abt, C., Bade, S. D., Birk, L., and Harries, S. (2001). Parametric hull form design-a step towards one week ship design. *8th International Symposium on Practical Design of Ships and Other Floating Structures. PRADS 2001, Shanghai, China.*

Armijo, L. (1966). Minimization of functions having lipschitz continuous first partial derivatives. *Pacific journal of Mathematics*, 16.

Bagheri, H., Ghassemi, H., and Dehghanian, A. (2014). Optimizing the seakeeping performance of ship hull forms using genetic algorithm. *The International Journal on Marine Navigation and Safety of Sea Transportation*, 8(1).

Bailey, T. C. and Gatrell, A. C. (1995). *Interactive Spatial Data Analysis*. Longman, Harlow.

Banks, J. B., Phillips, A. B., Bull, P. W., and Turnock, S. R. (2010). Rans simulations of the multiphase flow around the kcs hull form. *A Workshop on Numerical Ship Hydrodynamics. Gothenburg.*

Borkowski, J. J. (2016). Response surface methodology, stat 578, section 6.

Chun, H. (2010). Hull form parameterization technique with local and global optimization algorithms. *Proceedings of MARTEC.*

Grigoropoulos, G. J. (2004). Hull form optimization for hydrodynamic performance. *Marine Technology*, 41(4):167–182.

Han, S., Lee, S. L., and Choi, Y. B. (2012). Hydrodynamic hull form optimization using parametric models. *Journal of Marine Science and Technology*, 17:1–17.

Harries, S. (1998). *Parametric design and hydrodynamic optimization of ship hull forms*. PhD thesis, Technische Universitöt, Germany.

Hedar, A.-R. (2004). *Studies on Metaheuristics for Continuous Global Optimization Problems*. PhD thesis, Kyoto University, Japan.

Hollister, S. M. (1996). Automatic hull variation and optimization. *Meeting of the New England Section of the Society of Naval Architects and Marine Engineers*.

Hsiao, C. T. (1996). *Numerical study of the tip vortex flow over a finite-span hydrofoil*. PhD thesis, Pennsylvania State University, USA.

Isaaks, E. H. and Srivastava, M. R. (1989). *An Introduction to Applied Geostatistics*. Oxford University Press, New York.

Janson, C. and Larsson, L. (1997). A method for the optimization of ship hulls from a resistance point of view. *Twenty-First Symposium on Naval Hydrodynamics*.

Kim, H. and Yang, C. (2010a). Hull form optimization for reduced resistance and improved seakeeping via practical designed-oriented cfd tools. *9th International Conference on Hydrodynamics, October 11-15, Shanghai, China*.

Kim, H. and Yang, C. (2010b). A new surface modification approach for cfd-based hull form optimization. *9th International Conference on Hydrodynamics, October 11-15, Shanghai, China*.

Kim, H. and Yang, C. (2011). Hydrodynamic optimization of multihull ships. *11th International Conference on Fast Sea Transportation*.

Kim, H. and Yang, C. (2013). Design optimization of bulbous bow and stern end bulb for reduced drag. *Proceedings of the Twenty-third(2013) International Offshore and Polar engineering*.

Kim, H., Yang, C., Löhner, R., and Noblesse, F. (2008). A practical hydrodynamic optimization tool for design of a monohull ship. *Proceedings of Eighteenth International Offshore and Polar Engineering Conference*.

Kim, H., Yang, C., and Nobless, F. (2010). Hull form optimization for reduced resistance and improved seakeeping via practical designed-oriented cfd tools. *Grand Challenges in Modeling and Simulation*.

Kratch, A. M. (1978). *Design of Bulbous Bows*. SNAME Transactions.

Lackenby, H. (1950). On the systematic geometrical variation of ship forms. *R.I.N.A 92(1950), p. 289*.

Larsson, L., Stern, F., and Bertram, V. (2003). Benchmarking of computational fluid dynamics for ship flows: the gothenburg 2000 workshop. *Journal of Ship Research*, 47.

Mahmood, S. and Huang, D. (2012). Computational fluid dynamics based bulbous bow optimization using a genetic algorithm. *Journal of Marine Science and Technology*, 11:286–294.

Markov, N. E. and Suzuki, K. (2001). Hull form optimization by shift and deformation of ship sections. *Journal of Ship Research*, 45(3):197–204.

Matulja, D. and Dejhalla, R. (2013). Optimization of the ship hull hydrodynamic characteristics in calm water.

Mckay, M. D., Beckman, R. J., and Conover, W. J. (1979). A comparison of three methods for selecting values of input variables in the analysis of output from a computer code. *Technometrics*, pages 239–245.

NIST (2016). Single response: Path of steepest ascent.

Nowacki, H., Bloor, M., and Oleksiewicz, B. (1995). *Computational Geometry for Ships*. World Scientific Pub Co Inc.

Park, D. W. and Choi, H. J. (2013). Hydrodynamic hull form design using an optimization technique. *International Journal of Ocean System Engineering*, 3(1):1–9.

Peng, H., Qiu, W., and Ni, S. (2014). Wave pattern and resistance prediction for ships of full form. *Ocean Engineering*, 87:162–173.

Piegl, L. and Tiller, W. (1997). *The NURBS Book*. Springer.

Ping, Z., Zhu, D., and Leng, W. (2008). Parametric aproach to design of hull forms. *Journal of Hydrodynamics*, 20:804–810.

Press, W. H., Teukolsky, S. A., Vetterling, W. T., P, F. B., and M, M. (1996). *Numerical Recipes in Fortran 90*. Cambridge University Press.

Rao, S. S. (1996). *Engineering Optimization: Theory and Practice*. A Wiley-Interscience Publication.

Raska, P. and Ulrych, Z. (2014). Testing optimization methods on discrete event simulation models and testing functions. *24th DAAAM International Symposium on Intelligent Manufacturing and Automation*, 69:768–777.

Rogers, D. F. (1980). B-spline surfaces for ship hull design. *ACM 1980*.

Saha, G. K., Suzuki, K., and Kai, H. (2004). Hydrodynamic optimization of ship hull forms in shallow water. *Journal of Marine Science and Technology*, 9:51–62.

Sakata, S., Ashida, F., and Zako, M. (2004). An efficient algorithm for kriging approximation and optimization with large-scale sampling data. *Computer Methods in Applied Mechanics and Engineering*, pages 385–404.

Tarafder, M. S. and Suzuki, K. (2008). Numerical calculation of free-surface potential flow around a ship using the modified rankine source panel method. *Journal of Ocean Engineering*, 35:536–544.

Taubin, G. (1995). Curve and surface smoothing without shrinkage. *Fifth International Conference on Computer Vision*, pages 852 – 857.

Appendix A

Typical IGES Format

A typical format of IGES file is provided here.

```
START RECORD GO HERE.                                                    S      1
                                                                         S      2
1H,,1H;,,                                                                G      1
44HC:\Users\AMHL\Desktop\Nizam\MV Arctic\qw.igs,                          G      2
26HRhinoceros ( Sep 28 2012 ),31HTrout Lake IGES 012 Sep 28 2012,        G      3
32,38,6,308,15,                                                          G      4
,                                                                        G      5
1.0D0,2,2HMM,1,0.254D0,13H160113.211323,                                 G      6
0.001D0,                                                                 G      7
1079.984605334227D0,                                                     G      8
,                                                                        G      9
,                                                                        G     10
10,0,13H160113.211323;                                                   G     11
     314       1       0       0       0       0       0       000000200D      1
     314       0       1       1       0       0       0   COLOR       0D      2
     406       2       0       0       1       0       0       000000300D      3
     406       0      -1       1       3       0       0LEVELDEF       0D      4
     406       3       0       0       0       0       0       000010300D      5
     406       0       0       1      15       0       0 NAMETXT       0D      6
     128       4       0       0       1       0       0       000000000D      7
     128       0      -1      14       0       0       0 TrimSrf       0D      8
314,0.0,0.0,0.0,20HRGB(   0,   0,   0 );                          0000001P      1
406,2,1,7HDefault;                                                 0000003P      2
406,1,7HTrimSrf;                                                   0000005P      3
128,2,2,2,2,0,0,1,0,0,0.0D0,0.0D0,0.0D0,298.486898873367D0,        0000007P      4
298.486898873367D0,298.486898873367D0,0.0D0,0.0D0,0.0D0,           0000007P      5
37.56465848382695D0,37.56465848382695D0,37.56465848382695D0,       0000007P      6
1.0D0,1.0D0,1.0D0,1.0D0,1.0D0,1.0D0,1.0D0,1.0D0,1.0D0,             0000007P      7
-1070.772389144024D0,376.546074090295D0,-35.19991D0,               0000007P      8
-933.4519358463474D0,325.2108445661814D0,-35.19929308862278D0,     0000007P      9
-782.77232417594D0,354.3405623075698D0,-35.19952966770001D0,       0000007P     10
-1079.984605334227D0,376.5461223656893D0,-62.06749880314137D0,     0000007P     11
-927.69493423164O9D0,306.1567115593063D0,-66.44606016511236D0,     0000007P     12
-782.7765663923691D0,377.8986286453096D0,-63.45630906876161D0,     0000007P     13
-1070.41468810065D0,376.5462306616424D0,-55.01726833296978D0,      0000007P     14
-933.6753739785805D0,376.4047599367322D0,-56.61591912937411D0,     0000007P     15
-782.7723241743563D0,376.5393258751362D0,-56.00285001718849D0,     0000007P     16
0.0D0,298.486898873367D0,0.0D0,37.56465848382695D0,0,1,5;          0000007P     17
S0000002G0000011D0000008P0000017                                         T      1
```

Appendix B

MAPS Resistance Input

A typical format of MAPS resistance input for ship geometry is provided here.

```
! Characteristics of hull
   5796        5625           1           0           0
      1          45         125

! List of Points
    1      0.500001      0.000000      0.000000
    2      0.499256      0.000000     -0.000385
    3      0.498478      0.000000     -0.000779
   ... ... ... ...
   ... ... ... ...

 5794     -0.493182      0.000000     -0.049899
 5795     -0.492178      0.000000     -0.051206
 5796     -0.491142      0.000000     -0.052490

 ! List of Panels
      1       1      47      48       2
      2       2      48      49       3
      3       3      49      50       4
   ... ... ... ...
   ... ... ... ...

   5623    5747    5793    5794    5748
   5624    5748    5794    5795    5749
   5625    5749    5795    5796    5750
```